Topics in the transport theory of quark–gluon plasma

Stanislaw Mrówczyński
Soltan Institute for Nuclear Studies, ul. Hoża 69, PL—00-681 Warsaw, Poland;
Institute of Physics, Pedagogical University, ul. Konopnickiej 15, PL—25-406 Kielce, Poland[*)]

Fiz. Élem. Chastits At. Yadra **30**, 954–991 (July–August 1999)

A few topics of the transport theory of quark–gluon plasma are reviewed. A derivation of the transport equations from the underlaying dynamical theory is discussed within the ϕ^4 model. Peculiarities of the kinetic equations of quarks and gluons are considered, and the plasma (linear) response to the color field is studied. The chromoelectric tensor permeability is found, and the plasma oscillations are discussed. Finally, the filamentation instability in the strongly anisotropic parton system from ultrarelativistic heavy-ion collisions is discussed in detail.
 [S1063-7796(99)00404-0]

1. INTRODUCTION

The quark–gluon plasma (QGP) is a macroscopic system of deconfined quarks and gluons. The very existence of QGP at a sufficiently high temperature and/or baryon density is basically an unavoidable consequence of quantum chromodynamics (QCD), which is a dynamical theory of strong interactions (see, e.g., Ref. 1). The plasma has been present in the early Universe and presumably can be found in compact stellar objects. Of particular interest, however, is the generation of QGP in relativistic heavy-ion collisions, which has been actively studied theoretically and experimentally[2] for over ten years. The lifetime of the plasma produced, if indeed it is produced, in these collisions is not much longer than the characteristic time scale of parton processes.[1)] Therefore, QGP can achieve, in the best case, only a quasi-equilibrium state, and studies of nonequilibrium phenomena are crucial to discriminate the characteristic features of QGP.

The transport or kinetic theory provides a natural framework to study systems out of thermodynamical equilibrium. Although the theory was initiated more than a century ago (Boltzmann derived his famous equation in 1872), the theory is still under vital development. Application of Boltzmann's ideas to systems which are relativistic and have a quantum nature face difficulties which have so far been overcome only partially. For a review, see the monograph of Ref. 3. In the case of the quark–gluon plasma, specific difficulties appear due to the non-Abelian dynamics of the system. Nevertheless, the transport-theory approach to QGP is making fast progress, and some interesting results have already been found.

The aim of this article is to review a few topics of the QGP transport theory. The first problem is how to derive the transport equations of quarks and gluons. Since QCD is the underlying dynamical theory, these equations should be deduced from QCD. However, the kinetic theory of quarks and gluons has been successfully derived from QCD only in the mean-field or collisionless limit.[4,5] The derivation of the collision terms is still an open question. We discuss here the issue within a dynamical model which is much simpler than QCD. Namely, we consider self-interacting scalar fields with a quartic interaction term. Then one can elucidate the essence of the derivation problem.

In Sec. 3 we present the transport equations for quarks and gluons obtained in the mean-field limit. The equations are supplemented with collision terms which are justified on a phenomenological basis. We briefly discuss the peculiarities of the transport theory of quarks and gluons and then consider the locally colorless plasma.[2)] The dynamical content of QCD enters here only through the cross sections of parton–parton interactions.

The characteristic features of QGP appear when the plasma is not locally colorless, and consequently it interacts with the chromodynamic mean field. The plasma response to such a field is discussed in Sec. 4, where the color-conductivity and chromoelectric-permeability tensors are found. We also analyze there the oscillations around the global thermodynamical equilibrium.

The parton momentum distribution is expected to be strongly anisotropic at the early stage of ultrarelativistic heavy-ion collisions. Then, the parton system can be unstable with respect to the specific plasma modes. In Sec. 5 we discuss in detail the mode which splits the parton system into color current filaments parallel to the beam direction. We show why the fluctuation which initiates the filamentation can be very large and explain the physical mechanism responsible for the fluctuation growth. Then, the exponentially growing mode is found as a solution of the respective dispersion equation. The characteristic time of development of the instability is estimated, and finally, the possibility of observing the color filamentation in nucleus–nucleus collisions at RHIC and LHC is considered.

In presenting the QGP transport theory we try to avoid model-dependent concepts, but we adopt the very crucial assumption that the plasma is perturbative, i.e., that the partons interact weakly with each other. As is well known, QGP becomes perturbative only at temperatures much greater than the QCD scale parameter $\Lambda \cong 200\,\mathrm{MeV}$; see, e.g., Ref. 6. However, it is believed that many results obtained in the framework of perturbative QCD can be extrapolated to the *nonperturbative* regime.

Throughout the article we use the units in which $c=k$

$=\hbar=1$. The metric tensor is diagonal with $g_{00}=-g_{11}=-g_{22}=-g_{33}=1$.

2. DERIVATION OF THE TRANSPORT EQUATION IN THE ϕ^4 MODEL

Transport equations can usually be derived by means of simple heuristic arguments similar to those used by Boltzmann when he formulated the kinetic theory of gases. However, such arguments are insufficient when one studies a system of complicated dynamics like the quark–gluon plasma governed by QCD. Then, one has to refer to a formal scheme to derive the transport equation directly from the underlying quantum field theory. The formal scheme is also needed to specify the limits of the kinetic approach. Indeed, the derivation shows the assumptions and approximations which lead to the transport theory, and hence the domain of its applicability can be established.

Until now the transport equations of the QCD plasma have been successfully derived in the mean-field limit,[4,5] and the structure of these equations is well understood.[4,5,7–10] In particular, it has been shown that in quasi-equilibrium these equations provide[5,8] the so-called hard thermal loops.[11] The collisionless transport equations can be applied to a variety of problems. However, one needs collision terms to discuss dissipative phenomena. In spite of some efforts[12–15] the general form of these terms in the transport equations of the quark–gluon plasma remains unknown. The QCD transport equations should also take into account particle creation and annihilation, which are entirely absent in the nonrelativistic atomic systems described by the Boltzmann equation. Particle production can occur as a result of particle collisions or the presence of strong fields, as in the Schwinger mechanism.[16] The latter phenomenon has been actively studied in the context of the quark–gluon transport theory; see, e.g., Refs. 17–22. However, one has had to refer to simplifying assumptions, such as the (quasi-)homogeneity of the field, to get tractable equations.

The so-called Schwinger–Keldysh[23,24] formulation of quantum field theory provides a very promising basis to derive the transport equation beyond the mean-field limit. Kadanoff and Baym[25] developed a technique for nonrelativistic quantum systems, which has been further generalized to relativistic ones.[14,26–35] We mention here only the papers which provide a more or less systematic analysis of the collision terms.

The derivation of the complete QCD transport equations appears to be a very difficult task. In particular, the treatment of massless fields such as gluons is troublesome. Apart from the well known infrared divergences which plague the perturbative expansion, there is a specific problem of nonequilibrium massless fields. The inhomogeneities in the system cause off-mass-shell propagation of particles, and then the perturbative analysis of the collision terms appears hardly tractable. More specifically, it appears very difficult, if possible at all, to express the field self-energy as the squared transition matrix element, and consequently we lose the probabilistic character of the kinetic theory. The problem is absent for massive fields when the system is assumed to be homogeneous at the inverse mass or Compton scale. This is a natural assumption within the transport theory, which anyway deals with quantities averaged over a certain scale, which can be identified with the Compton one. We have developed[36] a systematic approach to the transport of massless fields, which allows one to treat these fields in a very similar manner to massive ones. The basic idea is rather obvious. Fields which are massless in a vacuum gain an effective mass in a medium due to the interaction. Therefore, the minimal scale at which the transport theory works is not an inverse bare mass, which is infinite for massless fields, but the inverse effective one. The starting point of the perturbative computation should no longer be free fields, but must be interacting ones. In physical terms, we have postulated the existence of massive quasiparticles, and we look for their transport equation. We have successfully applied the method to massless scalar fields,[36] but the generalization to QCD is far from straightforward, owing to the much richer quasiparticle spectrum.

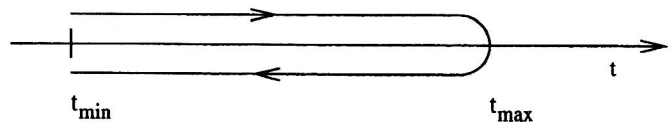

FIG. 1. The contour along the time axis for an evaluation of the operator expectation values.

To demonstrate the characteristic features of the transport-theory derivation, we discuss in this section the simplest nontrivial model, i.e., real massive fields with the Lagrangian density

$$\mathcal{L}(x)=\frac{1}{2}\partial^{\mu}\phi(x)\partial_{\mu}\phi(x)-\frac{1}{2}m^2\phi^2(x)-\frac{g}{4!}\phi^4(x). \tag{2.1}$$

The main steps of the derivation are the following. One defines a contour Green function with time arguments on a contour in the complex-time plane. This function, which is a key element of the Schwinger–Keldysh approach, satisfies the Dyson–Schwinger equation. Assuming macroscopic quasihomogeneity of the system, one performs a gradient expansion and a Wigner transformation. Then the pair of Dyson–Schwinger equations is converted into transport and mass-shell equations, both satisfied by the Wigner function. One further computes perturbatively the self-energy, which provides the Vlasov and the collisional terms of the transport equation. Finally, one defines the distribution function of the standard probabilistic interpretation and finds the transport equation satisfied by this function.

2.1. Green functions

The contour Green function is defined as

$$i\Delta(x,y)\overset{\text{def}}{=}\langle\tilde{T}\phi(x)\phi(y)\rangle,$$

where $\langle....\rangle$ denotes the ensemble average at time t_0 (usually identified with $-\infty$); $\tilde{T}$ is the time-ordering operation along the directed contour shown in Fig. 1. The parameter t_{max} is

shifted to $+\infty$ in the calculations. The time arguments are complex with an infinitesimal positive or negative imaginary part, which locates them on the upper or on the lower branch of the contour. The ordering operation is defined as

$$\tilde{T}\phi(x)\phi(y) \overset{\text{def}}{=} \Theta(x_0,y_0)\phi(x)\phi(y) + \Theta(y_0,x_0)\phi(y)\phi(x),$$

where $\Theta(x_0,y_0)$ equals 1 if x_0 succeeds y_0 on the contour, and equals 0 when x_0 precedes y_0.

If the field is expected to develop a finite expectation value, as happens when the symmetry is spontaneously broken, the contribution $\langle\phi(x)\rangle\langle\phi(y)\rangle$ is subtracted from the right-hand side of the equation defining the Green function; see, e.g., Refs. 30 and 31. Then one concentrates on the field fluctuations around the expectation values. Since $\langle\phi(x)\rangle$ is expected to vanish in models defined by the Lagrangians (2.1), we neglect this contribution in the Green-function definition.

We also use four other Green functions with real time arguments:

$$i\Delta^{>}(x,y) \overset{\text{def}}{=} \langle\phi(x)\phi(y)\rangle,$$

$$i\Delta^{<}(x,y) \overset{\text{def}}{=} \langle\phi(y)\phi(x)\rangle,$$

$$i\Delta^{c}(x,y) \overset{\text{def}}{=} \langle T^{c}\phi(x)\phi(y)\rangle,$$

$$i\Delta^{a}(x,y) \overset{\text{def}}{=} \langle T^{a}\phi(x)\phi(y)\rangle,$$

where $T^c(T^a)$ prescribes (anti-)chronological time ordering:

$$T^{c}\phi(x)\phi(y) \overset{\text{def}}{=} \Theta(x_0-y_0)\phi(x)\phi(y) + \Theta(y_0-x_0)\phi(y)\phi c(x),$$

$$T^{a}\phi(x)\phi(y) \overset{\text{def}}{=} \Theta(y_0-x_0)\phi(x)\phi(y) + \Theta(x_0-y_0)\phi(y)\phi(x).$$

These functions are related to the contour Green functions in the following manner:

$\Delta^c(x,y)\equiv\Delta(x,y)$ for x_0,y_0 from the upper branch,

$\Delta^a(x,y)\equiv\Delta(x,y)$ for x_0,y_0 from the lower branch,

$\Delta^{>}(x,y)\equiv\Delta(x,y)$ for x_0 from the upper branch and y_0 from the lower one,

$\Delta^{<}(x,y)\equiv\Delta(x,y)$ for x_0 from the lower branch and y_0 from the upper one.

It appears convenient to introduce the retarded (+) and advanced (−) Green functions

$$\Delta^{\pm}(x,y) \overset{\text{def}}{=} \pm(\Delta^{>}(x,y)-\Delta^{<}(x,y))\Theta(\pm x_0 \mp y_0). \quad (2.2)$$

One easily finds several identities which directly follow from the definitions and relate the Green functions to each other.

$\Delta^c(x,y)$ describes the propagation of a disturbance in which a single particle is added to the many-particle system at the space-time point y and is then removed from it at the space-time point x. An antiparticle disturbance is propagated backward in time. The meaning of $\Delta^a(x,y)$ is analogous, but particles are propagated backward in time, and antiparticles forward. In the zero-density limit $\Delta^c(x,y)$ coincides with the Feynman propagator.

The physical meaning of the functions $\Delta^{>}(x,y)$ and $\Delta^{<}(x,y)$ is more transparent when one considers the Wigner transform defined as

$$\Delta^{\lessgtr}(X,p) \overset{\text{def}}{=} \int d^4u\, e^{ipu}\Delta^{\lessgtr}\left(X+\frac{1}{2}u, X-\frac{1}{2}u\right). \quad (2.3)$$

Then the free-field energy–momentum tensor averaged over the ensemble can be expressed as

$$t_0^{\mu\nu}(X) \overset{\text{def}}{=} -\frac{1}{4}\langle\phi(x)\overleftrightarrow{\partial}^{\mu}\overleftrightarrow{\partial}^{\nu}\phi(x)\rangle = \int\frac{d^4p}{(2\pi)^4}p^{\mu}p^{\nu}i\Delta^{<}(X,p).$$

One recognizes the standard form of the energy–momentum tensor in the kinetic theory with the function $i\Delta^{<}(X,p)$, giving the density of particles with four-momentum p at a space-time point X. Therefore, $i\Delta^{<}(X,p)$ can be treated as a quantum analog of the classical distribution function. Indeed, the function $i\Delta^{<}(X,p)$ is Hermitian. However, it is not positive definite, and the probabilistic interpretation is only approximately valid. One should also observe that, in contrast to the classical distribution functions, $i\Delta^{<}(X,p)$ can be nonzero for off-mass-shell four-momenta.

2.2. Equations of motion

The Dyson–Schwinger equations satisfied by the contour Green function are

$$[\partial_x^2+m^2]\Delta(x,y) = -\delta^{(4)}(x,y) + \int_C d^4x'\,\Pi(x,x')\Delta(x',y), \quad (2.4)$$

$$[\partial_y^2+m^2]\Delta(x,y) = -\delta^{(4)}(x,y) + \int_C d^4x'\,\Delta(x,x')\Pi(x',y), \quad (2.5)$$

where $\Pi(x,y)$ is the self-energy; the integration over x_0' is performed on the contour, and the function $\delta^{(4)}(x,y)$ is defined on the contour as

$$\delta^{(4)}(x,y) = \begin{cases} \delta^{(4)}(x-y) & \text{for } x_0,y_0 \text{ from the upper branch,} \\ 0 & \text{for } x_0,y_0 \text{ from different branches,} \\ -\delta^{(4)}(x-y) & \text{for } x_0,y_0 \text{ from the lower branch.} \end{cases}$$

Let us split the self-energy into three parts:

$$\Pi(x,y) = \Pi_{\delta}(x)\delta^{(4)}(x,y) + \Pi^{>}(x,y)\Theta(x_0,y_0) + \Pi^{<}(x,y)\Theta(y_0,x_0).$$

As we shall see later, Π_{δ} provides a dominant contribution to the mean field, while $\Pi^{\lessgtr}$ determines the collision terms of the transport equations.

With the help of the retarded and advanced Green functions (2.2) and the retarded and advanced self-energies defined in an analogous way, Eqs. (2.4) and (2.5) can be rewritten as

$$[\partial_x^2+m^2-\Pi_\delta(x)]\Delta^{\gtrless}(x,y)=\int d^4x'[\Pi^{\gtrless}(x,x')\Delta^-(x',y) +\Pi^+(x,x')\Delta^{\gtrless}(x',y)], \quad (2.6)$$

$$[\partial_y^2+m^2-\Pi_\delta(y)]\Delta^{\gtrless}(x,y)=\int d^4x'[\Delta^{\gtrless}(x,x')\Pi^-(x',y) +\Delta^+(x,x')\Pi^{\gtrless}(x',y)], \quad (2.7)$$

where all time integrations run from $-\infty$ to $+\infty$.

2.3. Towards the transport equation

The transport equations are derived under the assumption that the Green functions and the self-energies depend weakly on the sum of their arguments and that they are significantly different from zero only when the difference of their arguments is close to zero. For homogeneous systems, the dependence on $X=(x+y)/2$ drops out, solely because of the translational invariance, and $\Delta(x,y)$ depends only on $u=x-y$. For weakly inhomogeneous, or quasihomogeneous systems, the Green functions and self-energies are assumed to vary slowly with X. We additionally assume that the Green functions and self-energies are strongly peaked near $u=0$, which means that the correlation length is short.

We will now convert Eqs. (2.6) and (2.7) into transport and mass-shell equations by implementing the above approximation and performing the Wigner transformation (2.3) for all the Green functions and self-energies. This is done by means of translation rules such as

$$\int d^4x' f(x,x')g(x',y)\to f(X,p)g(X,p) +\frac{i}{2}\left[\frac{\partial f(X,p)}{\partial p_\mu}\frac{\partial g(X,p)}{\partial X^\mu} -\frac{\partial f(X,p)}{\partial X^\mu}\frac{\partial g(X,p)}{\partial p_\mu}\right],$$

$$h(x)g(x,y)\to h(X)g(X,p)-\frac{i}{2}\frac{\partial h(X)}{\partial X^\mu}\frac{\partial g(X,p)}{\partial p_\mu},$$

$$\partial_x^\mu f(x,y)\to\left(-ip^\mu+\frac{1}{2}\partial^\mu\right)f(X,p).$$

Here $\partial^\mu\equiv\partial/\partial X_\mu$, and the functions $f(x,y)$ and $g(x,y)$ satisfy the assumptions discussed above. The function $h(x)$ is assumed to be weakly dependent on x.

The kinetic theory deals only with averaged system characteristics. Thus, one usually assumes that the system is homogeneous on the scale of the Compton wavelength of the quasiparticles. In other words, the characteristic length of inhomogeneities is assumed to be much larger than the inverse mass of the quasiparticles. Therefore, we impose the condition

$$|\Delta^{\gtrless}(X,p)|\gg\left|\frac{1}{m^2}\partial^2\Delta^{\gtrless}(X,p)\right|, \quad (2.8)$$

which leads to the quasiparticle approximation. The requirement (2.8) renders the off-shell contributions to the Green functions $\Delta^{\gtrless}$ negligible. Thus, we deal with quasiparticles having on-mass-shell momenta.

Applying the translation rules and the quasiparticle approximation to Eqs. (2.6) and (2.7), we obtain

$$\left[p^\mu\partial_\mu-\frac{1}{2}\partial_\mu\Pi_\delta(X)\partial_p^\mu\right]\Delta^{\gtrless}(X,p) =\frac{i}{2}(\Pi^>(X,p)\Delta^<(X,p)-\Pi^<(X,p)\Delta^>(X,p)) -\frac{1}{4}\{\Pi^{\gtrless}(X,p),\ \Delta^+(X,p)+\Delta^-(X,p)\} -\frac{1}{4}\{\Pi^+(X,p)+\Pi^-(X,p),\ \Delta^{\gtrless}(X,p)\}, \quad (2.9)$$

$$[-p^2+m^2-\Pi_\delta(X)]\Delta^{\gtrless}(X,p) =\frac{1}{2}(\Pi^{\gtrless}(X,p)(\Delta^+(X,p)+\Delta^-(X,p))+(\Pi^+(X,p) +\Pi^-(X,p))\Delta^{\gtrless}(X,p)) +\frac{i}{4}\{\Pi^>(X,p),\ \Delta^<(X,p)\} -\frac{i}{4}\{\Pi^<(X,p),\ \Delta^>(X,p)\}, \quad (2.10)$$

where we have introduced the Poisson-like bracket defined as

$$\{C(X,p),D(X,p)\}\equiv\frac{\partial C(X,p)}{\partial p_\mu}\frac{\partial D(X,p)}{\partial X^\mu} -\frac{\partial C(X,p)}{\partial X^\mu}\frac{\partial D(X,p)}{\partial p_\mu}.$$

One recognizes Eq. (2.9) as a transport equation, while Eq. (2.10) is a so-called mass-shell equation. We write these equations in a more compact form:

$$\{p^2-m^2+\Pi_\delta(X)+\mathrm{Re}\,\Pi^+(X,p),\ \Delta^{\gtrless}(X,p)\} =i(\Pi^>(X,p)\Delta^<(X,p)-\Pi^<(X,p)\Delta^>(X,p)) -\{\Pi^{\gtrless}(X,p),\ \mathrm{Re}\,\Delta^+(X,p)\}, \quad (2.11)$$

$$[p^2-m^2+\Pi_\delta(X)+\mathrm{Re}\,\Pi^+(X,p)]\Delta^{\gtrless}(X,p) =-\Pi^{\gtrless}(X,p)\mathrm{Re}\,\Delta^+(X,p)-\frac{i}{4}\{\Pi^>(X,p),\ \Delta^<(X,p)\} +\frac{i}{4}\{\Pi^<(X,p),\ \Delta^>(X,p)\}. \quad (2.12)$$

The gradient terms on the right-hand sides of Eqs. (2.11) and (2.12) are usually neglected.[30,31]

We introduce the spectral function A defined as

$$A(x,y) \overset{\text{def}}{=} \langle [\phi(x),\phi(y)] \rangle = i\Delta^{>}(x,y) - i\Delta^{<}(x,y),$$

where $[\phi(x),\phi(y)]$ denotes the field commutator. Owing to the equal-time commutation relations

$$[\phi(t,\mathbf{x}),\phi(t,\mathbf{y})]=0, \quad [\dot{\phi}(t,\mathbf{x}),\phi(t,\mathbf{y})]=-i\delta^{(3)}(\mathbf{x}-\mathbf{y}),$$

with the dot denoting the time derivative, the Wigner-transformed spectral function satisfies the two identities

$$\int \frac{dp_0}{2\pi} A(X,p)=0, \quad \int \frac{dp_0}{2\pi} p_0 A(X,p)=1.$$

From the transport and mass-shell equations (2.11) and (2.12) one immediately finds equations satisfied by $A(X,p)$:

$$\{p^2-m^2+\Pi_\delta(X)+\mathrm{Re}\,\Pi^+(X,p),\ A(X,p)\} = 2\{\mathrm{Im}\,\Pi^+(X,p),\mathrm{Re}\,\Delta^+(X,p)\}, \tag{2.13}$$

$$[p^2-m^2+\Pi_\delta(X)+\mathrm{Re}\,\Pi^+(X,p)]A(X,p) = 2\,\mathrm{Im}\,\Pi^+(X,p)\mathrm{Re}\,\Delta^+(X,p). \tag{2.14}$$

One solves the algebraic equation (2.14) as

$$A(X,p) = \frac{2\,\mathrm{Im}\,\Pi^+(X,p)}{(p^2-m^2+\Pi_\delta(X)+\mathrm{Re}\,\Pi^+(X,p))^2+(\mathrm{Im}\,\Pi^+(X,p))^2}. \tag{2.15}$$

Then it can be shown that the function (2.15) solves Eq. (2.13) as well. The spectral function of the free fields can be found as

$$A_0(X,p)=2\pi\delta(p^2-m^2)(\Theta(p_0)-\Theta(-p_0)).$$

Since $\mathrm{Re}\,\Pi^+$ determines the quasiparticle effective mass, and $\mathrm{Im}\,\Pi^+$ determines its width, the spectral function characterizes the quasiparticle properties.

2.4. Perturbative expansion

As discussed in Refs. 28, 29, and 37, for example, the contour Green functions admit a perturbative expansion very similar to that known from the vacuum field theory, with essentially the same Feynman rules. However, the time integrations run not from $-\infty$ to $+\infty$, but along the contour shown in Fig. 1. The right turning point of the contour ($t_{\max}$) must be above the largest time argument of the evaluated Green function. In practice, t_0 is shifted to $-\infty$, and ($t_{\max}$) to $+\infty$. The second difference is the appearance of tadpoles, i.e., loops formed by single lines, which give zero contribution in the vacuum case. A tadpole corresponds to a Green function with two equal space-time arguments. Since the Green function $\Delta(x,y)$ is not well defined for $x=y$, we ascribe the function $-i\Delta^{<}(x,x)$ to each tadpole. The rest of the Feynman rules can be taken from the textbook of Bjorken and Drell.[38]

The lowest-order contribution to the self-energy, which is associated with the graph in Fig. 2 is

$$\Pi(x,y)=-\frac{ig}{2}\delta^{(4)}(x,y)\Delta_0^{<}(x,x),$$

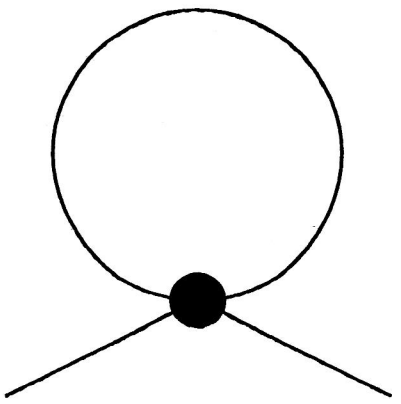

FIG. 2. The lowest-order diagram of the self-energy.

giving

$$\Pi_\delta(x)=-\frac{ig}{2}\Delta_0^{<}(x,x), \tag{2.16}$$

and

$$\Pi^{>}(x,y)=\Pi^{<}(x,y)=0.$$

The one-particle irreducible g^2 contributions to the self-energy are shown in Fig. 3. The contribution corresponding to diagram 3a can be easily computed. However, it is purely

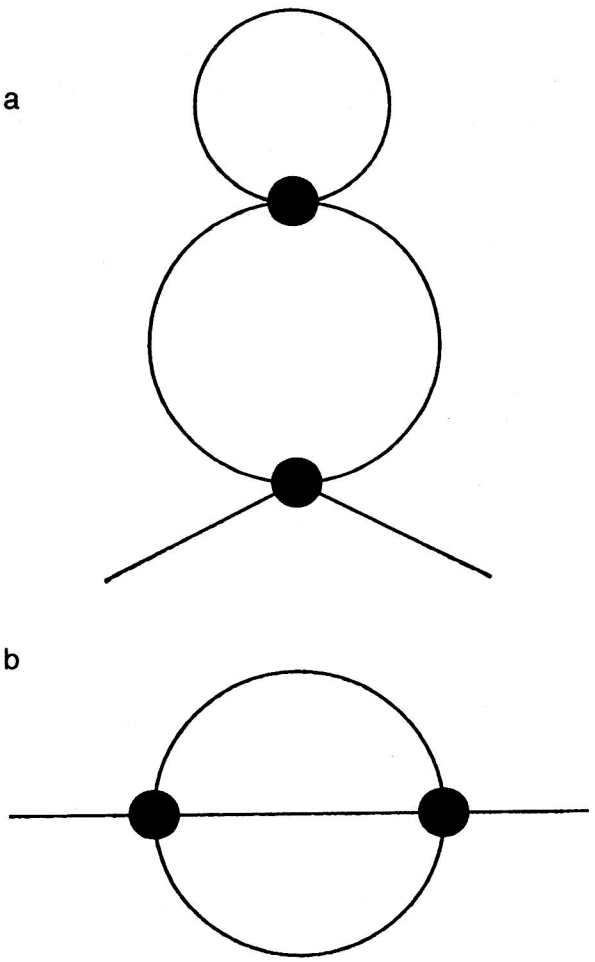

FIG. 3. The second-order diagrams of the self-energy.

real, and the only effect of this contribution is a higher-order modification of the mean-field term. Thus, we do not consider this diagram, but instead we analyze the contribution 3b, which provides a qualitatively new effect. It gives the contour self-energy

$$\Pi_c(x,y)=\frac{g^2}{6}\Delta_0(x,y)\Delta_0(y,x)\Delta_0(x,y),$$

and consequently

$$\Pi^{\gtrless}(x,y)=\frac{g^2}{6}\Delta_0^{\gtrless}(x,y)\Delta_0^{\lessgtr}(y,x)\Delta_0^{\gtrless}(x,y). \tag{2.17}$$

2.5. Distribution function and transport equation

The distribution function $f(X,p)$ is defined as

$$\Theta(p_0)i\Delta^<(X,p)=\Theta(p_0)A(X,p)f(X,p),$$

where $A(X,p)$ is the spectral function (2.15). Then one finds[36] that

$$i\Delta^>(X,p)=\Theta(p_0)A(X,p)(f(X,p)+1) -\Theta(-p_0)A(X,p)f(X,-p), \tag{2.18}$$

$$i\Delta^<(X,p)=\Theta(p_0)A(X,p)f(X,p) -\Theta(-p_0)A(X,p)(f(X,-p)+1). \tag{2.19}$$

There is a very important property of $\Delta^{\gtrless}$ expressed in the form (2.18) and (2.19). Namely, if the Green functions $\Delta^{\gtrless}$ satisfy the transport equation (2.11) and the spectral function solves Eq. (2.14), the mass-shell equation for $\Delta^{\gtrless}$, i.e., Eq. (2.12), is satisfied *automatically* in the zeroth order of the gradient expansion. We note that the quasiparticle dispersion relation is found as a solution of the equation

$$p^2-m^2+\Pi_\delta(X)+\mathrm{Re}\,\Pi^+(X,p)=0. \tag{2.20}$$

The distribution function f satisfies the transport equation which can be obtained from Eq. (2.11) for $\Delta^>$ or $\Delta^<$. After using Eq. (2.13), one finds

$$\begin{aligned}&A(X,p)\{p^2-m^2+\mathrm{Re}\,\Pi^+(X,p),f(X,p)\}\\&\quad=iA(X,p)(\Pi^>(X,p)f(X,p)-\Pi^<(X,p)\\&\qquad\times(f(X,p)+1))+if(X,p)\{\Pi^>(X,p),\ \mathrm{Re}\,\Delta^+(X,p)\}\\&\qquad-i(f(X,p)+1)\{\Pi^<(X,p),\ \mathrm{Re}\,\Delta^+(X,p)\},\end{aligned} \tag{2.21}$$

where $p_0>0$. We have also used here the following property of the Poisson-like brackets:

$$\{A,BC\}=\{A,B\}C+\{A,C\}B.$$

The left-hand side of Eq. (2.21) is a straightforward generalization of the drift term of the standard relativistic transport equation. Computing the Poisson-like bracket and imposing the mass-shell constraint, one finds the familiar structure

$$\begin{aligned}&\frac{1}{2}\Theta(p_0)\{p^2-m^2+\mathrm{Re}\,\Pi^+(X,p),f(X,p)\}\\&\quad=E_p\left(\frac{\partial}{\partial t}+\mathbf{v}\nabla\right)f(X,p)-\nabla\,\mathrm{Re}\,\Pi^+(X,p)\\&\qquad\times\nabla_p f(X,p),\end{aligned}$$

where the velocity $\mathbf{v}$ is equal to $\partial E_p/\partial\mathbf{p}$ with the (positive) energy E_p being the solution of the dispersion equation (2.20).

Let us now analyze the right-hand side of Eq. (2.21). The collision terms are provided by the self-energies (2.17). Since the quasiparticles of interest are narrow ($m^2+\mathrm{Re}\,\Pi^+ \gg \mathrm{Im}\,\Pi^+$), we take into account only those terms contributing to $\Pi^{\gtrless}$ which are nonzero for on-mass-shell momenta. The other terms are negligibly small.[36] Then the first term on the right-hand side of the transport equation (2.21) is very similar to the standard collision term[3] of the Nordheim[39] (or Uehling–Uhlenbeck[40]) form. Indeed,

$$\begin{aligned}&i(\Pi^>(X,p)f(X,p)-\Pi^<(X,p)(f(X,p)+1))\\&\quad=\frac{g^2}{2}\int\frac{d^4kA_k^+}{(2\pi)^4}\frac{d^4qA_q^+}{(2\pi)^4}\frac{d^4rA_r^+}{(2\pi)^4}(2\pi)^4\delta^{(4)}(p+q-k-r)\\&\qquad\times((f^p+1)(f^q+1)f^kf^r-f^pf^q(f^k+1)(f^r+1)),\end{aligned}$$

where $A_k^+\equiv\Theta(k_0)A(X,k)$ and $f^k\equiv f(X,k)$. The last two terms on the right-hand side of Eq. (2.21), which are neglected in the usual transport equation, are discussed in Ref. 36.

3. TRANSPORT EQUATIONS OF QUARKS AND GLUONS

In this section we introduce the gauge-dependent distribution functions of quarks and gluons. Then we discuss the transport equations satisfied by these functions. Finally, a very useful notion of locally colorless plasma is considered.

3.1. Distribution functions

The (anti)quark distribution function $Q(p,x)$ [$\bar{Q}(p,x)$] is a Hermitian $N_c\times N_c$ matrix in color space [for the $SU(N_c)$ color group], where p denotes the quark four-momentum and x is the space-time coordinate.[41–43] The function transforms under local gauge transformations as

$$Q(p,x)\to U(x)Q(p,x)U^\dagger(x). \tag{3.1}$$

The color indices are suppressed here and in most cases below.

The gluon distribution function[44] is a Hermitian $(N_c^2-1)\times(N_c^2-1)$ matrix,[7] which transforms as

$$G(p,x)\to M(x)G(p,x)M^\dagger(x), \tag{3.2}$$

where

$$M_{ab}(x)=\mathrm{Tr}[\tau_aU(x)\tau_bU^\dagger(x)],$$

in which τ_a, with $a=1,\ldots,N_c^2-1$, are the $SU(N_c)$ group generators in the fundamental representation. One sees that, in contrast to the distribution functions known from the physics of atomic gases, the distribution functions of quarks

and gluons have no simple probabilistic interpretation, owing to the gauge dependence. This is, however, not surprising if one realizes that the question about the probability of finding, let us say, a red quark in a phase-space cell centered around (p,x) is not physical, since the color of a quark can be changed by means of a gauge transformation.

It follows from the transformation laws (3.1) and (3.2) that the traces of the distribution functions are gauge-independent, and consequently they can have a familiar probabilistic interpretation. Indeed, the probability of finding a quark of arbitrary color in a cell (p,x) has physical meaning, since it is gauge-independent. Quantities which are color (gauge) independent, like the baryon current b^μ or the energy–momentum tensor $t^{\mu\nu}$, are expressed entirely in terms of the traces of the distribution functions:

$$b^\mu(x)=\frac{1}{3}\int\frac{d^3p}{(2\pi)^3E}p^\mu[\mathrm{Tr}[Q(p,x)]-\mathrm{Tr}[\bar{Q}(p,x)]],$$

$$t^{\mu\nu}(x)=\int\frac{d^3p}{(2\pi)^3E}p^\mu p^\nu[\mathrm{Tr}[Q(p,x)]+\mathrm{Tr}[\bar{Q}(p,x)]+\mathrm{Tr}[G(p,x)]],$$

where E is the quark or gluon energy. Both quarks and gluons are assumed to be massless, and their spin is treated as an internal degree of freedom. The spin structure of the distribution functions and the respective transport equations have been discussed in Refs. 9 and 10.

The color current, which is a gauge-dependent quantity, is expressed in terms of not only the traces of the distribution functions, but also the functions themselves. In $N_c\times N_c$ matrix notation, the current takes the form

$$j^\mu(x)=-\frac{1}{2}g\int\frac{d^3p}{(2\pi)^3E}p^\mu\Big[Q(p,x)-\bar{Q}(p,x)-\frac{1}{N_c}\mathrm{Tr}[Q(p,x)-\bar{Q}(p,x)]+2i\tau_a f_{abc}G_{bc}(p,x)\Big], \tag{3.3}$$

where g is the QCD coupling constant and the f_{abc} are the structure constants of the $SU(N_c)$ group. In the adjoint representation the color current (3.3) is

$$j_a^\mu(x)=-g\int\frac{d^3p}{(2\pi)^3E}p^\mu[\mathrm{Tr}[\tau_a(Q(p,x)-\bar{Q}(p,x))]+if_{abc}G_{bc}(p,x)],$$

where we have used the equality $\mathrm{Tr}(\tau_a\tau_b)=\frac{1}{2}\delta_{ab}$.

3.2. Transport equations

The distribution functions of the quarks and gluons satisfy the following set of transport equations (Refs. 4, 7, and 41–44):

$$p^\mu D_\mu Q(p,x)+gp^\mu\frac{\partial}{\partial p_\nu}\frac{1}{2}\{F_{\mu\nu}(x),Q(p,x)\}=C[Q,\bar{Q},G],$$

$$p^\mu D_\mu\bar{Q}(p,x)-gp^\mu\frac{\partial}{\partial p_\nu}\frac{1}{2}\{F_{\mu\nu}(x),\bar{Q}(p,x)\}=\bar{C}[Q,\bar{Q},G],$$

$$p^\mu\mathcal{D}_\mu G(p,x)+gp^\mu\frac{\partial}{\partial p_\nu}\frac{1}{2}\{\mathcal{F}_{\mu\nu}(x),G(p,x)\}=C_g[Q,\bar{Q},G], \tag{3.4}$$

where $\{...,...\}$ denotes the anticommutator; D_μ and $\mathcal{D}_\mu$ are the covariant derivatives, which act as

$$D_\mu=\partial_\mu-ig[A_\mu(x),...],\quad \mathcal{D}_\mu=\partial_\mu-ig[\mathcal{A}_\mu(x),...],$$

where A_μ and $\mathcal{A}_\mu$ are the mean-field four-potentials, defined as

$$A^\mu(x)=A_a^\mu(x)\tau_a,\quad \mathcal{A}_{ab}^\mu(x)=-if_{abc}A_c^\mu(x).$$

$F_{\mu\nu}$ and $\mathcal{F}_{\mu\nu}$ are the mean-field stress tensors, with a color-index structure analogous to that of the four-potentials. The mean field is generated by the color current (3.3), and the corresponding equation is

$$D_\mu F^{\mu\nu}(x)=j^\nu(x). \tag{3.5}$$

C, $\bar{C}$, and C_g are the collision terms, which vanish in the collisionless limit, i.e., when the plasma evolution is dominated by the mean-field effects.[3] As already mentioned, the collision terms of the QGP kinetic equations have not yet been systematically derived, and their structure remains obscure. The situation is simpler in the case of the colorless plasma discussed in the next section. We note that the set of transport equations (3.4) and (3.5) is covariant with respect to the gauge transformations (3.1) and (3.2).

3.3. Colorless plasma

The evolution of the system of quarks and gluons towards thermodynamical equilibrium tends to neutralize the color charges. It is expected[13] that after a short period of time the plasma becomes locally colorless, and the color current and the mean field $F^{\mu\nu}$ vanish. Then the distribution functions of the quarks and gluons are proportional to the unit matrices in the color space. Specifically,

$$Q_{ij}(p,x)=\frac{1}{N_c}\delta_{ij}q(p,x),\quad i,j=1,...,N_c,$$

$$\bar{Q}_{ij}(p,x)=\frac{1}{N_c}\delta_{ij}\bar{q}(p,x),$$

$$G_{ab}(p,x)=\frac{1}{N_c^2-1}\delta_{ab}g(p,x),\quad a,b=1,...,N_c^2-1.$$

It can be seen that the distribution functions of the colorless plasma are gauge-invariant.

The transport equations of the colorless plasma are essentially simplified. Indeed, by taking the trace of Eqs. (3.4) one finds

$$p^\mu\partial_\mu q(x,p)=c[q,\bar{q},g],$$

$$p^\mu\partial_\mu\bar{q}(x,p)=\bar{c}[q,\bar{q},g],$$

$$p^\mu\partial_\mu g(x,p)=c_g[q,\bar{q},g], \tag{3.6}$$

where $c\equiv\mathrm{Tr}\,C$, $\bar{c}\equiv\mathrm{Tr}\,\bar{C}$, and $c_g\equiv\mathrm{Tr}\,C_g$. Because the trace of a commutator is zero, the covariant derivatives reduce to the normal ones in (3.6).

In the case of a colorless plasma the color charges can be treated as internal degrees of freedom of the quarks and gluons, and it is sufficient to work with the color-averaged quantities, which are gauge-independent. Then one can imitate the dynamics of the colorless plasma with a non-gauge field-theory model such as ϕ^4. Then the collision terms are of the Nordheim[39] (or Uehling–Uhlenbeck[40]) form, as discussed in the preceding section. Therefore, even without knowing the collision terms C, $\bar{C}$, and C_g, we expect that the corresponding terms of the colorless plasma, c, $\bar{c}$, and c_g, which represent the binary collisions, are

$$
\begin{aligned}
c[q,\bar{q},g]=\int \frac{d^3p_2}{(2\pi)^3E_2}\frac{d^3p_3}{(2\pi)^3E_3}\frac{d^3p_4}{(2\pi)^3E_4}\Big[&\frac{1}{2}[q_3q_4(1-q_1)\\
&\times(1-q_2)-q_1q_2(1-q_3)(1-q_4)]W_{qq\to qq}\\
&\times(p_3,p_4|p_1,p_2)+[q_3\bar{q}_4(1-q_1)(1-\bar{q}_2)\\
&-q_1\bar{q}_2(1-q_3)(1-\bar{q}_4)]W_{q\bar{q}\to q\bar{q}}(p_3,p_4|p_1,p_2)\\
&+[q_3g_4(1-q_1)(1+g_2)-q_1g_2(1-q_3)(1+g_4)]\\
&\times W_{qg\to qg}(p_3,p_4|p_1,p_2)+[g_3g_4(1-q_1)\\
&\times(1-\bar{q}_2)-q_1\bar{q}_2(1+g_3)(1+g_4)]\\
&\times W_{q\bar{q}\to gg}(p_3,p_4|p_1,p_2)\Big]
\end{aligned}
\tag{3.7}
$$

with analogous expressions for $\bar{c}[\bar{q},q,g]$ and $c_g[g,q,\bar{q},]$. We have used here the abbreviations $q_1\equiv q(x,p_1)$, $q_2\equiv q(x,p_2)$, etc. Furthermore, $p_1\equiv p$. The coefficient $\frac{1}{2}$ in the first term of the right-hand side of Eq. (3.7) is required to avoid the double counting of identical particles. The quantities like $W_{qg\to qg}(p_3,p_4|p_1,p_2)$, which correspond to quark–gluon scattering, are equal to the square of the respective matrix element multiplied by the energy–momentum conserving δ function. We note that the collision terms must satisfy the relations

$$
\int \frac{d^3p}{(2\pi)^3E}[c[q,\bar{q},g]-\bar{c}[q,\bar{q},g]]=0,
$$

$$
\int \frac{d^3p}{(2\pi)^3E}p^\mu[c[q,\bar{q},g]+\bar{c}[q,\bar{q},g]+c_g[q,\bar{q},g]]=0,
$$

in order to be consistent with baryon-number and energy–momentum conservation.

In a variety of applications one uses the collision terms in the relaxation-time approximation, i.e.,

$$
\begin{aligned}
c&=\nu p_\mu u^\mu(x)(q^{eq}(p,x)-q(p,x)),\\
\bar{c}&=\bar{\nu}p_\mu u^\mu(x)(\bar{q}^{eq}(p,x)-\bar{q}(p,x)),\\
c_g&=\nu_g p_\mu u^\mu(x)(g^{eq}(p,x)-g(p,x)),
\end{aligned}
\tag{3.8}
$$

where ν, $\bar{\nu}$, and ν_g are the collision frequencies and u^μ is the hydrodynamic four-velocity which defines the local rest frame of the quark–gluon system. The equilibrium distribution functions are

$$
q^{eq}(p,x)=\frac{2N_fN_c}{\exp(\beta^\mu(x)p_\mu-\beta(x)\mu(x))+1},
$$

$$
\bar{q}^{eq}(p,x)=\frac{2N_fN_c}{\exp(\beta^\mu(x)p_\mu+\beta(x)\mu(x))+1},
$$

$$
g^{eq}(p,x)=\frac{2(N_c^2-1)}{\exp(\beta^\mu(x)p_\mu)-1},
$$

where $\beta^\mu(x)\equiv\beta(x)u^\mu(x)$ and $\beta(x)\equiv T^{-1}(x)$; $T(x)$ and $\mu(x)$ are the local temperature and quark chemical potential, respectively; N_f is the number of quark flavors. Spin, flavor, and color are treated here as internal degrees of freedom.

4. PLASMA COLOR RESPONSE

In this section we discuss how the plasma, which is colorless, homogeneous, and stationary, responds to small fluctuations of the color.

4.1. Linear-response analysis

The distribution functions are assumed to be of the form

$$
\begin{aligned}
Q_{ij}(p,x)&=n(p)\delta_{ij}+\delta Q_{ij}(p,x),\\
\bar{Q}_{ij}(p,x)&=\bar{n}(p)\delta_{ij}+\delta\bar{Q}_{ij}(p,x),\\
G_{ab}(p,x)&=n_g(p)\delta_{ab}+\delta G_{ab}(p,x),
\end{aligned}
\tag{4.1}
$$

where the functions describing the deviation from the colorless state are assumed to be much smaller than the respective colorless functions. The same is assumed for the momentum gradients of these functions.

Substituting (4.1) into (3.3), one gets

$$
\begin{aligned}
j^\mu(x)=-\frac{1}{2}g\int\frac{d^3p}{(2\pi)^3E}p^\mu\Big[&\delta Q(p,x)-\delta\bar{Q}(p,x)\\
&-\frac{1}{N_c}\mathrm{Tr}[\delta Q(p,x)-\delta\bar{Q}(p,x)]\\
&+2i\tau_a f_{abc}\delta G_{bc}(p,x)\Big].
\end{aligned}
\tag{4.2}
$$

We see that the current occurs as a result of the deviation of the system from the colorless state. When the system becomes neutral, there is no current and one expects that there is no mean field. Therefore, we linearize Eq. (3.5) with respect to the four-potential:

$$
\partial_\mu F^{\mu\nu}(x)=j^\nu(x)
$$

with $F^{\mu\nu}=\partial^\mu A^\nu-\partial^\nu A^\mu$. It should be stressed here that the linearization procedure does not cancel all non-Abelian effects. The gluon–gluon coupling, which is of essentially non-Abelian character, is included because the gluons contribute to the color current (4.2). We also observe that in the linearized theory the color current is conserved (owing to the antisymmetry of $F^{\mu\nu}$), i.e., $\partial_\mu j^\mu=0$. Finally, we note that, as shown in Ref. 5, the semiclassical QCD transport theory effectively incorporates a resummation over the so-called hard thermal loops.[11]

Now we substitute the distribution functions (4.1) into the transport equations (3.4) with the collision terms (3.8). Linearizing the equations with respect to δQ, $\delta\bar{Q}$, and δG, one gets

$$(p^\mu\partial_\mu+\nu p_\mu u^\mu)\,\delta Q(p,x)=-gp^\mu F_{\mu\nu}(x)\frac{\partial n(p)}{\partial p_\nu}+\nu p_\mu u^\mu(n^{eq}(p)-n(p)),$$

$$(p^\mu\partial_\mu+\bar\nu p_\mu u^\mu)\,\delta\bar Q(p,x)=gp^\mu F_{\mu\nu}(x)\frac{\partial \bar n(p)}{\partial p_\nu}+\bar\nu p_\mu u^\mu(\bar n^{eq}(p)-\bar n(p)),$$

$$(p^\mu\partial_\mu+\nu_g p_\mu u^\mu)\,\delta G(p,x)=-gp^\mu \mathcal{F}_{\mu\nu}(x)\frac{\partial n_g(p)}{\partial p_\nu}+\nu_g p_\mu u^\mu(n_g^{eq}(p)-n_g(p)). \tag{4.3}$$

In performing the linearization, one should remember that A^μ is of the order of δQ. Treating the chromodynamical field as an external one, Eqs. (4.3) are easily solved:

$$\delta Q(p,x)=-g\int d^4x'\,\Delta_p(x-x')\left[p^\mu F_{\mu\nu}(x')\frac{\partial n(p)}{\partial p_\nu}-\nu p_\mu u^\mu(n^{eq}(p)-n(p))\right],$$

$$\delta\bar Q(p,x)=g\int d^4x'\,\Delta_p(x-x')\left[p^\mu F_{\mu\nu}(x')\frac{\partial \bar n(p)}{\partial p_\nu}+\bar\nu p_\mu u^\mu(\bar n^{eq}(p)-\bar n(p))\right],$$

$$\delta G(p,x)=-g\int d^4x'\,\Delta_p(x-x')\left[p^\mu \mathcal{F}_{\mu\nu}(x')\frac{\partial n_g(p)}{\partial p_\nu}-\nu_g p_\mu u^\mu(n_g^{eq}(p)-n_g(p))\right], \tag{4.4}$$

where $\Delta_p(x)$ is the Green function of the kinetic operator with the collision term in the relaxation-time approximation,

$$\Delta_p(x)=E^{-1}\Theta(t)e^{-\nu' t}\delta^{(3)}(\mathbf{x}-\mathbf{v}t),$$

in which t is the zeroth component of x, $x^\mu\equiv(t,\mathbf{x})$, $\mathbf{v}\equiv\mathbf{p}/E$, and $\nu'\equiv\nu p^\mu u_\mu$; in the plasma rest frame, $\nu'=\nu$.

Substituting the solutions (4.4) into Eq. (4.2) and performing a Fourier transformation with respect to the x variable, we get

$$j^\mu(k)=\sigma^{\mu\rho\lambda}(k)F_{\rho\lambda}(k) \tag{4.5}$$

with the color conductivity tensor expressed as

$$\sigma^{\mu\rho\lambda}(k)=i\frac{g^2}{2}\int\frac{d^3p}{(2\pi)^3E}\left[\frac{p^\mu p^\rho}{p^\sigma(k_\sigma+i\nu u_\sigma)}\times\frac{\partial n(p)}{\partial p_\lambda}+\frac{p^\mu p^\rho}{p^\sigma(k_\sigma+i\bar\nu u_\sigma)}\frac{\partial\bar n(p)}{\partial p_\lambda}+\frac{2N_c p^\mu p^\rho}{p^\sigma(k_\sigma+i\nu_g u_\sigma)}\frac{\partial n_g(p)}{\partial p_\lambda}\right]. \tag{4.6}$$

If the colorless state of the plasma is isotropic, which is the case for the global equilibrium, one finds that $\sigma^{\mu\rho\lambda}(k)=\sigma^{\mu\rho}(k)u^\lambda$, and Eq. (4.5) takes the more familiar form of Ohm's law, which in the plasma rest frame becomes

$$j^\alpha(k)=\sigma^{\alpha\beta}(k)E^\beta(k),$$

where the indices $\alpha,\beta,\gamma=1,2,3$ label the space axes and $E^\alpha(k)$ is the α component of the chromoelectric vector. The conductivity tensor describes the response of the QGP to the chromodynamical field. Within the approximation used here it is a color scalar (no color indices) or, equivalently, is proportional to the unit matrix in the color space. In the next subsections we will extract information about the QGP contained in $\sigma^{\mu\rho\lambda}(k)$.

4.2. Chromoelectric permeability

Let us introduce, as in electrodynamics, the polarization vector $\mathbf{P}(x)$ defined as

$$\operatorname{div}\mathbf{P}(x)=-\rho(x),\quad \frac{\partial}{\partial t}\mathbf{P}(x)=\mathbf{j}(x), \tag{4.7}$$

where ρ and $\mathbf{j}$ are the time-like and space-like components, respectively, of the color-induced four-current $j^\mu=(\rho,\mathbf{j})$. The definition (4.7) is self-consistent only when the color current is conserved, not covariantly conserved. This is just the case of the linear-response approach. Further, we define the chromoelectric induction vector $\mathbf{D}(x)$,

$$\mathbf{D}(x)=\mathbf{E}(x)+\mathbf{P}(x), \tag{4.8}$$

and the chromoelectric permeability tensor, which relates the Fourier-transformed $\mathbf{D}$ and $\mathbf{E}$ fields,

$$D^\alpha(k)=\epsilon^{\alpha\beta}(k)E^\beta(k), \tag{4.9}$$

where $\alpha,\beta=1,2,3$. Since the conductivity tensor (4.6) is a color-scalar, the permeability tensor is a color-scalar as well.

Using the definitions (4.7)–(4.9), one easily finds that

$$\epsilon^{\alpha\beta}(k)=\delta^{\alpha\beta}-\frac{i}{\omega}\sigma^{\alpha 0\beta}(k)-\frac{i}{\omega^2}[k^\gamma\sigma^{\alpha\beta\gamma}(k)-k^\gamma\sigma^{\alpha\gamma\beta}(k)] \tag{4.10}$$

with $\sigma^{\alpha\gamma\beta}(k)$ given by Eq. (4.6); ω is the time-like component of the wave four-vector $k^\mu\equiv(\omega,\mathbf{k})$. For an isotropic plasma the last two terms in Eq. (4.10) vanish. Substituting the conductivity tensor (4.6) into Eq. (4.10), we get the permeability tensor in the plasma rest frame:

$$\epsilon^{\alpha\beta}(k)=\delta^{\alpha\beta}+\frac{g^2}{2\omega}\int\frac{d^3p}{(2\pi)^3}\left[\frac{v^\alpha}{\omega-\mathbf{k}\cdot\mathbf{v}+i\nu}\frac{\partial n(p)}{\partial p_\gamma}+\frac{v^\alpha}{\omega-\mathbf{k}\cdot\mathbf{v}+i\bar\nu}\frac{\partial\bar n(p)}{\partial p_\gamma}+2N_c\frac{v^\alpha}{\omega-\mathbf{k}\cdot\mathbf{v}+i\nu_g}\frac{\partial n_g(p)}{\partial p_\gamma}\right]\times\left[\left(1-\frac{\mathbf{k}\cdot\mathbf{v}}{\omega}\right)\delta^{\gamma\beta}+\frac{k^\gamma v^\beta}{\omega}\right]. \tag{4.11}$$

In the case of an isotropic plasma the permeability tensor can be expressed as

$$\epsilon^{\alpha\beta}(k)=\epsilon_T(k)(\delta^{\alpha\beta}-k^\alpha k^\beta/\mathbf{k}^2)+\epsilon_L(k)k^\alpha k^\beta/\mathbf{k}^2,$$

with the longitudinal and transverse permeability functions given by

$$\epsilon_L(k)=1+\frac{g^2}{2\omega\mathbf{k}^2}\int\frac{d^3p}{(2\pi)^3}\left[\frac{\mathbf{k}\cdot\mathbf{v}k^\gamma}{\omega-\mathbf{k}\cdot\mathbf{v}+i\nu}\frac{\partial n(p)}{\partial p_\gamma}+\frac{\mathbf{k}\cdot\mathbf{v}k^\gamma}{\omega-\mathbf{k}\cdot\mathbf{v}+i\bar{\nu}}\frac{\partial\bar{n}(p)}{\partial p_\gamma}+\frac{\mathbf{k}\cdot\mathbf{v}k^\gamma}{\omega-\mathbf{k}\cdot\mathbf{v}+i\nu_g}\frac{\partial n_g(p)}{\partial p_\gamma}\right], \tag{4.12}$$

$$\epsilon_T(k)=1+\frac{g^2}{2\omega}\int\frac{d^3p}{(2\pi)^3}\left[\frac{1}{\omega-\mathbf{k}\cdot\mathbf{v}+i\nu}\frac{\partial n(p)}{\partial p_\gamma}+\frac{1}{\omega-\mathbf{k}\cdot\mathbf{v}+i\bar{\nu}}\frac{\partial\bar{n}(p)}{\partial p_\gamma}+\frac{1}{\omega-\mathbf{k}\cdot\mathbf{v}+i\nu_g}\frac{\partial n_g(p)}{\partial p_\gamma}\right]\times\left[v^\gamma-\frac{\mathbf{k}\cdot\mathbf{v}k^\gamma}{\mathbf{k}^2}\right]. \tag{4.13}$$

Because the QCD equations within the linear-response approach coincide (apart from a trivial matrix structure) with those of electrodynamics, the dispersion relations of the plasma oscillations, or of plasmons, are those of electrodynamics, and they take the form[45,46]

$$\det|\mathbf{k}^2\delta^{\alpha\beta}-k^\alpha k^\beta-\omega^2\epsilon^{\alpha\beta}(k)|=0. \tag{4.14}$$

The relation (4.14) takes a simpler form for an isotropic plasma. Namely,

$$\epsilon_L(k)=0,\quad \epsilon_T(k)=\mathbf{k}^2/\omega^2. \tag{4.15}$$

The dispersion relations determine the plasma waves which can be propagate in the medium. Specifically, the plane wave with $\omega(\mathbf{k})$ satisfying the dispersion equation (4.14) automatically solves the sourceless Maxwell equations in a medium. In "quantum" language, the dispersion equation gives the relation between the energy and the momentum of the quasiparticle excitations. In the case of plasma these are the transverse and longitudinal plasmons.

There are three classes of solutions of Eq. (4.14). Those with purely real ω are stable—the wave amplitude is constant in time. If the imaginary part of the frequency is negative, the oscillations are damped—the amplitude decreases in time. Of particular interest are the solutions with positive $\mathrm{Im}\,\omega$, corresponding to so-called plasma instabilities—oscillations with an amplitude that grows exponentially in time.

The permeability tensor in the static limit ($\omega\to 0$) provides information about the plasma response to constant fields. Computing $\epsilon_L(\omega=0,\mathbf{k})$ for an equilibrium collisionless plasma, one finds

$$\epsilon_L(\omega=0,\mathbf{k})=1+\frac{m_D^2}{\mathbf{k}^2},$$

where m_D is the Debye mass, which for a baryonless plasma of massless quarks and gluons is given by

$$m_D^2=\frac{g^2T^2(N_f+2N_c)}{6}. \tag{4.16}$$

The chromoelectric potential of a static point-like source embedded in the plasma, which is given by[46,47]

$$A_0(\mathbf{x})=\frac{g}{4\pi|\mathbf{x}|}\exp(-m_D|\mathbf{x}|),$$

is screened at the distance $1/m_D$.

Since the parton density is $\sim T^3$, one finds from Eq. (4.16) that the number of partons in the Debye sphere (the sphere of radius equal to the screening length) is $\sim 1/g^3$. It is much greater than unity if the plasma is *perturbative*, i.e., when $1/g\gg 1$. A large parton number in the Debye sphere justifies, in particular, the use of the mean field to describe the QGP. We also mention that the ultrarelativistic perturbative plasma is automatically ideal, i.e., the average parton interaction energy, which is $\sim g^2/\langle r\rangle$, where $\langle r\rangle\sim T^{-1}$ is the average interparticle distance, is much smaller than the parton thermal energy, which is $\sim T$. This is not the case for the nonrelativistic electron plasma. In that case the screening length is (see, e.g., Refs. 46 and 47)

$$m_D^2=e^2\frac{n_e}{T},$$

where n_e is the electron density,[4)] which is independent of the temperature. It can be seen that the smallness of the coupling constant does not guarantee that the nonrelativistic plasma is ideal. This occurs when the number of electrons in the Debye sphere is large, i.e., when $T^{3/2}\gg e^3 n_e^{1/2}$.

4.3. Oscillations around the global equilibrium

Substituting the equilibrium distribution functions (Fermi–Dirac for quarks and Bose–Einstein for gluons) into Eqs. (4.13) and (4.14), one finds the permeability functions ϵ_L and ϵ_T, which for a collisionless ($\nu=\bar{\nu}=\nu_g=0$) and baryonless ($\mu=0$) plasma of massless partons can be computed analytically as

$$\epsilon_L=1+\frac{3\omega_0^2}{k^2}\left[1-\frac{\omega}{2k}\left[\ln\left|\frac{k+\omega}{k-\omega}\right|-i\pi\Theta(k-\omega)\right]\right], \tag{4.17}$$

$$\epsilon_T=1-\frac{3\omega_0^2}{2k^2}\left[1-\left(\frac{\omega}{2k}-\frac{k}{2\omega}\right)\left[\ln\left|\frac{k+\omega}{k-\omega}\right|-i\pi\Theta(k-\omega)\right]\right], \tag{4.18}$$

where $k\equiv|\mathbf{k}|$ and ω_0 is the plasma frequency, given by

$$\omega_0^2=\frac{g^2T^2(N_f+2N_c)}{18}. \tag{4.19}$$

We see that for $\omega>k$ the dielectric functions (4.17) and (4.18) are purely real, i.e., there are no dissipative processes.

Substituting (4.17) and (4.18) into (4.15), one finds the dispersion relation for the longitudinal mode (the chromoelectric field parallel to the wave vector) in the form

$$\omega^2=\begin{cases}\omega_0^2+\frac{3}{5}k^2 & \text{for } \omega_0\gg k,\\ k^2(1+4\exp(-2-2k^2/3\omega_0^2)) & \text{for } \omega_0\ll k,\end{cases}$$

and

$$\omega^2=\begin{cases}\omega_0^2+\frac{6}{5}k^2 & \text{for } \omega_0\gg k,\\ \frac{3}{2}\omega_0^2+k^2 & \text{for } \omega_0\ll k\end{cases}$$

for the transverse mode (the chromoelectric field perpendicular to the wave vector). Because the longitudinal and transverse oscillations are time-like ($\omega^2>k^2$), the phase velocity of the waves is greater than the velocity of light. For this reason, Landau damping is absent. As is well known, Landau damping is due to collisionless energy transfer from the wave to the plasma particles, whose velocity is equal to the wave phase velocity.[47]

The oscillations of the collisionless QGP around the global equilibrium have been studied by means of the transport theory in several papers (Refs. 7, 48, and 51–53). The problem has also been discussed in Refs. 49 and 50, using a specific variant of the QGP theory with the classical color.[41,54] In the above presentation we have followed Ref. 7. The dispersion relations given above agree with those found in finite-temperature QCD in the one-loop approximation; see, e.g., Refs. 6 and 55–57.

Let us now consider the dielectric function with nonzero equilibration rates. As before, the partons are massless and the plasma is baryonless, which means that $\nu=\bar{\nu}$. Then one can easily evaluate the integrals (4.13) and (4.14) for $\omega\gg k$, $\omega\gg\nu$, and $\omega\gg\nu_g$. The results are[7]

$$\omega^2=\omega_0^2-\zeta^2+\frac{3}{4}\phi^2+\frac{3}{5}k^2, \quad \gamma=\frac{1}{2}\phi$$

for the longitudinal mode, and

$$\omega^2=\omega_0^2-\zeta^2+\frac{3}{4}\phi^2+\frac{6}{5}k^2, \quad \gamma=\frac{1}{2}\phi$$

for the transverse one; ω and γ denote the real and imaginary part, respectively, of the complex frequency; ϕ and ζ are parameters related to the equilibration rates:

$$\phi=\nu\frac{N_f}{N_f+2N_c}+\nu_g\frac{2N_c}{N_f+2N_c},$$

$$\zeta^2=\nu^2\frac{N_f}{N_f+2N_c}+\nu_g^2\frac{2N_c}{N_f+2N_c}. \tag{4.20}$$

We see that, when compared with the collisionless plasma, the frequency of the oscillations is smaller and the oscillations are damped. To find the numerical value of the damping rate—the plasma oscillation decrement γ, the equilibration rates (ν and ν_g) have to be estimated.

If ν or ν_g is identified with the mean free flight time controlled by the binary collisions, the equilibration rate is of the order $g^4\ln(1/g)$. However, in the relativistic plasma there is another damping mechanism: plasmon decay into a quark–antiquark or gluon–gluon pair. It is easy to see that, even in the limit of massless quarks, decay into gluons is much more probable than that into quarks.[7,57] Let us consider the decay of a plasmon of zero momentum. The phase-space volume of the decay final state is proportional to

$$(1\mp n^{eq}(\omega_0/2))^2, \tag{4.21}$$

where the upper sign refers to quarks, and the lower one to gluons. Since the plasma frequency (4.19) is much smaller than the temperature in the perturbative plasma, the factor (4.21) can be expanded as

$$(1-n^{eq}(\omega_0/2))^2\cong 1/4+\omega_0/8T,$$

$$(1+n^{eq}(\omega_0/2))^2\cong 4T^2/\omega_0^2.$$

It can be seen that decay into gluons is more probable than that into quarks by a factor of order g^{-2} (Ref. 57).

Using the standard rules of finite-temperature field theory, one easily finds (see e.g., Ref. 7) the width of a zero-momentum plasmon due to decay into gluons:

$$\Gamma_d=\frac{g^2N_c}{2^4 3\pi}\omega_0(1+n^{eq}(\omega_0/2))^2\cong\frac{gN_cT}{2^{3/2}\pi(N_f+2N_c)^{1/2}},$$

which is the same for longitudinal and transverse plasmons. However, Γ_d cannot be identified with the plasmon equilibration rate Γ, because the plasmon decays are partially compensated by the plasmon formation processes. As was shown in Ref. 58 (see also Ref. 57), the formation rate Γ_f is related to Γ_d as

$$\Gamma_f=\exp(-\omega_0/T)\Gamma_d\cong(1-\omega_0/T)\Gamma_d.$$

Since the equilibration rate of the plasmon is $\Gamma=\Gamma_d-\Gamma_f$ (Ref. 58), one finds[57]

$$\Gamma\cong\frac{g^2N_cT}{12\pi}. \tag{4.22}$$

We note that Γ_d and Γ_f are of the order of g, while Γ is of the order of g^2. Since there is a preferred reference frame—the rest frame of the thermostat, the plasmon decay width is not a Lorentz scalar. Therefore, the result (4.22) is valid only for zero-momentum or approximately long-wave plasmons.

Substituting ν_g equal to (4.22) and $\nu=0$ into Eq. (4.20), one estimates the decrement of the oscillation damping as

$$\gamma\cong\frac{g^2}{12\pi}\frac{N_c^2}{N_f+2N_c}T. \tag{4.23}$$

Although $\nu=0$, the damping rate depends on the number of quark flavors. This seems to be in agreement with physical intuition. When the number of quark flavors is increased, the inertia of the system is also increased, and consequently the time needed to damp the oscillations is longer. However, Eq. (4.23) disagrees [by a factor $2N_c/(N_f+2N_c)$] with the result from Ref. 57, where γ is equal to (4.22). Unfortunately, the discrepancy cannot be resolved within the relaxation-time approximation, and a more elaborate analysis is needed.

5. FILAMENTATION INSTABILITY

In the near future nucleus–nucleus collisions will be studied experimentally at the accelerators of a new generation: the Relativistic Heavy-Ion Collider (RHIC) at Brookhaven and the Large Hadron Collider (LHC) at CERN. The collision energy will be larger by one or two orders of magnitude than for one of the currently operating machines. Copious production of partons, mainly gluons due to hard and semihard processes, is expected in the heavy-ion collisions in this new energy domain.[59,60] Thus, one is dealing with the many-parton system at an early stage of the collision. The system is on average locally colorless, but random fluctuations can break the neutrality. Since the system is initially far from equilibrium, specific color fluctuations can

grow exponentially in time and then noticeably influence the evolution of the system. While the very existence of such instabilities, similar to those known from the electron–ion plasma (see, e.g., Ref. 61), is fairly obvious and was mentioned long ago,[62] it is far less trivial to find those instabilities which are relevant for the parton system produced in ultrarelativistic heavy-ion collisions.

It has been argued that a system of two interpenetrating beams of nucleons[63,64] or partons[65–69] is unstable with respect to the so-called filamentation or Weibel instability.[70] However, such a system appears to be rather unrealistic from the experimental point of view. More recently, we have argued[71–73] that the filamentation can occur under weaker conditions which are very probable for heavy-ion collisions at RHIC and LHC. Instead of two streams of partons, it appears to be sufficient to assume a strongly anisotropic momentum distribution. We systematically review the whole problem here.

5.1. Fluctuation spectrum

We start with a discussion of how the unstable modes are initiated. Specifically, we show that the fluctuations, which act as seeds of the filamentation, are *large*—much larger than in the equilibrium plasma. Since the system of interest is far from equilibrium, the fluctuations are not determined by the chromodielectric permeability tensor discussed in the preceding subsection. The fluctuation–dissipation theorem does not hold in such a case. Thus, we derive the color-current correlation function which provides the fluctuation spectrum.

The QGP is assumed to be on average locally colorless, homogeneous, and stationary. Therefore, the distribution functions averaged over the ensemble are of the form

$$\langle Q_{ij}(t,\mathbf{x},\mathbf{p})\rangle = \delta^{ij} n(\mathbf{p}), \quad \langle \bar{Q}_{ij}(t,\mathbf{x},\mathbf{p})\rangle = \delta^{ij}\bar{n}(\mathbf{p}),$$

$$\langle G_{ab}(t,\mathbf{x},\mathbf{p})\rangle = \delta^{ab} n_g(\mathbf{p}),$$

which give the zero average color current.

We study the fluctuations of the color current, generalizing a well-known approach to the fluctuating electric current.[61] For a system of noninteracting quarks and gluons we have derived (in the classical limit) the following expression for the current correlation tensor:

$$M^{\mu\nu}_{ab}(t,\mathbf{x}) \overset{\text{def}}{=} \langle j^{\mu}_a(t_1,\mathbf{x}_1) j^{\nu}_b(t_2,\mathbf{x}_2)\rangle = \frac{1}{8} g^2 \delta^{ab} \int \frac{d^3p}{(2\pi)^3} \frac{p^{\mu}p^{\nu}}{E^2} f(\mathbf{p})\, \delta^{(3)}(\mathbf{x}-\mathbf{v}t), \tag{5.1}$$

where the effective parton distribution function $f(\mathbf{p})$ is equal to $n(\mathbf{p})+\bar{n}(\mathbf{p})+2N_c n_g(\mathbf{p})$, and $(t,\mathbf{x})\equiv(t_2-t_1,\mathbf{x}_2-\mathbf{x}_1)$. Owing to the average space-time homogeneity, the correlation tensor depends only on the difference $(t_2-t_1,\mathbf{x}_2-\mathbf{x}_1)$. The physical meaning of (5.1) is transparent. The space-time points $(t_1,\mathbf{x}_1)$ and $(t_2,\mathbf{x}_2)$ are correlated in the system of noninteracting particles if the particles go from $(t_1,\mathbf{x}_1)$ to $(t_2,\mathbf{x}_2)$. For this reason the delta function $\delta^{(3)}(\mathbf{x}-\mathbf{v}t)$ is present in (5.1). The momentum integral of the distribution function simply represents the summation over particles. The fluctuation spectrum is found as a Fourier transform of the tensor (5.1), i.e.,

$$M^{\mu\nu}_{ab}(\omega,\mathbf{k}) = \frac{1}{8} g^2 \delta^{ab} \int \frac{d^3p}{(2\pi)^3} \frac{p^{\mu}p^{\nu}}{E^2} f(\mathbf{p}) 2\pi\delta(\omega-\mathbf{k}\cdot\mathbf{v}). \tag{5.2}$$

When the system is in equilibrium, the fluctuations are given, according to the fluctuation–dissipation theorem, by the respective response function. For $f(\mathbf{p})$ equal to the classical equilibrium distribution function, one indeed finds the standard fluctuation–dissipation relation[61] valid in the g^2 order. For example,

$$M^{00}_{ab}(\omega,\mathbf{k}) = \delta^{ab} \frac{\mathbf{k}^2}{2\pi} \frac{T}{\omega} \operatorname{Im} \epsilon_L(\omega,\mathbf{k}),$$

where T is the temperature and ϵ_L represents the longitudinal part of the chromodielectric tensor (4.13).

5.2. Parton distributions

We model the parton momentum distribution at the early stage of an ultrarelativistic heavy-ion collision by two functions:

$$f(\mathbf{p}) = \frac{1}{2Y}\Theta(Y-y)\Theta(Y+y)h(p_\perp)\frac{1}{p_\perp \cosh y} \tag{5.3}$$

and

$$f(\mathbf{p}) = \frac{1}{2\mathcal{P}}\Theta(\mathcal{P}-p_\parallel)\Theta(\mathcal{P}+p_\parallel)h(p_\perp), \tag{5.4}$$

where y, $p_\parallel$, and $p_\perp$ denote the parton rapidity and the longitudinal and transverse momenta, respectively. The parton momentum distribution (5.3) corresponds to a rapidity distribution which is flat in the interval $(-Y,Y)$. The distribution (5.4) is flat for the longitudinal momentum, $-\mathcal{P}<p_\parallel<\mathcal{P}$. We do not specify the transverse momentum distribution $h(p_\perp)$, which is assumed to have the same shape for quarks and gluons, because it is sufficient for our considerations to demand that the distributions (5.3) and (5.4) are strongly elongated along the z axis, i.e., $e^Y \gg 1$ and $\mathcal{P} \gg \langle p_\perp\rangle$.

The QCD-based computations (see, e.g., Refs. 59 and 60) show that the rapidity distribution of partons produced at the early stage of heavy-ion collisions is essentially Gaussian with a width of about one to two units. When the distribution (5.3) simulates a Gaussian one, Y measures not the size of the "plateau" but rather the range over which the partons are spread. If one takes a Gaussian distribution with variance σ and the distribution (5.3) with the same variance, then $Y=\sqrt{3}\sigma$.

As already mentioned, the parton system described by the distribution functions (5.3) and (5.4) is assumed to be homogeneous and stationary. The applicability of this assumption is very limited because there is a correlation between the parton longitudinal momentum and its position, i.e., partons with very different momenta will find themselves in different regions of space shortly after the collision. However, one should remember that we are considering the parton system at a very early stage of the collision, soon after

the Lorentz-contracted ultrarelativistic nuclei traverse each other. At this stage partons are most copiously produced but do not have enough time to escape from each other. Thus, the assumption of homogeneity holds for a space-time domain of the longitudinal size, say, 2–3 fm, and lifetime 2–3 fm/c. As shown below, this time is long enough for the instability to occur.

5.3. Seeds of the filamentation

Let us now, calculate the correlation tensor (5.2) for the distribution functions (5.3) and (5.4). Owing to the symmetry $f(\mathbf{p})=f(-\mathbf{p})$ of these distributions, the tensor $M^{\mu\nu}$ is diagonal, i.e., $M^{\mu\nu}=0$ for $\mu\neq\nu$. Since the average parton longitudinal momentum is much larger than the transverse one, it obviously follows from Eq. (5.2) that the largest fluctuating current appears along the z axis. Therefore, we discuss the M^{zz} component of the correlation tensor. $M^{zz}(\omega,\mathbf{k})$ depends on the orientation of the vector $\mathbf{k}$ and there are two generic cases: $\mathbf{k}=(k_x,0,0)$ and $\mathbf{k}=(0,0,k_z)$. Inspection of Eq. (5.2) shows that the fluctuations with $\mathbf{k}=(k_x,0,0)$ are much larger than those with $\mathbf{k}=(0,0,k_z)$. Thus, let us consider $M^{zz}(\omega,k_x)$. Substituting the distributions (5.3) and (5.4) into (5.2), one finds after azimuthal integration that $M^{zz}_{ab}(\omega,k_x)$ reaches the maximal values for $\omega^2\ll k_x^2$. Thus, we compute M^{zz}_{ab} at $\omega=0$. Bearing in mind that $e^Y\gg 1$ and $\mathcal{P}\gg\langle p_\perp\rangle$, we get the following approximate expressions for the flat y and $p_\parallel$ distributions:

$$M^{zz}_{ab}(\omega=0,k_x)=\frac{1}{8}g^2\delta^{ab}\frac{e^Y}{Y}\frac{\langle\rho\rangle}{|k_x|}, \tag{5.5}$$

$$M^{zz}_{ab}(\omega=0,k_x)=\frac{1}{8}g^2\delta^{ab}\frac{\mathcal{P}}{\langle p_\perp\rangle}\frac{\langle\rho\rangle}{|k_x|}, \tag{5.6}$$

where $\langle\rho\rangle$ is the effective parton density, given for $N_c=3$ as

$$\langle\rho\rangle\equiv\int\frac{d^3p}{(2\pi)^3}f(\mathbf{p})=\frac{1}{4\pi^2}\int_0^\infty dp_\perp p_\perp h(p_\perp)$$
$$=\frac{1}{3}\langle\rho\rangle_{q\bar{q}}+\frac{3}{4}\langle\rho\rangle_g,$$

where $\langle\rho\rangle_{q\bar{q}}$ denotes the average density of quarks and antiquarks, and $\langle\rho\rangle_g$ is the same for gluons. For the flat $p_\parallel$ case we have also used the approximate equality

$$\int_0^\infty dp_\perp h(p_\perp)\cong\frac{1}{\langle p_\perp\rangle}\int_0^\infty dp_\perp p_\perp h(p_\perp)$$

to get the expression (5.6). It is instructive to compare the results (5.5) and (5.6) with the analogous result for the equilibrium plasma, which is

$$M^{zz}_{ab}(\omega=0,k_x)=\frac{\pi}{16}g^2\delta^{ab}\frac{\langle\rho\rangle}{|k_x|}.$$

We see that the current fluctuations in an anisotropic plasma are amplified by a large factor, which is e^Y/Y or $\mathcal{P}/\langle p_\perp\rangle$. With the estimated Y value of 2.5 for RHIC and 5.0 for LHC,[74] the amplification factor e^Y/Y is 4.9 and 29.7, respectively.

5.4. Filamentation mechanism

Following Ref. 75, we shall argue that the fluctuation which contributes to $M^{zz}_{ab}(\omega=0,k_x)$ grows in time. The form of the fluctuating current is

$$\mathbf{j}_a(x)=j_a\hat{\mathbf{e}}_z\cos(k_x x), \tag{5.7}$$

where $\hat{\mathbf{e}}_z$ is the unit vector in the z direction. Thus, there are current filaments of thickness $\pi/|k_x|$, with the current flowing in opposite directions in neighboring filaments. For the purpose of the qualitative argumentation presented here, the chromodynamics is treated as an eightfold electrodynamics. Then the magnetic field generated by the current (5.7) is

$$\mathbf{B}_a(x)=\frac{j_a}{k_x}\hat{\mathbf{e}}_y\sin(k_x x),$$

and the Lorentz force acting on the partons moving along the beam is

$$\mathbf{F}(x)=q_a\mathbf{v}\times\mathbf{B}_a(x)=-q_a v_z\frac{j_a}{k_x}\hat{\mathbf{e}}_x\sin(k_x x),$$

where q_a is the color charge. One observes (see Fig. 4) that the force distributes the partons in such a way that those which contribute positively to the current in a given filament are focused to the filament center, while those which contribute negatively are moved to the neighboring one. Thus, the initial current grows.

5.5. Dispersion equation

We analyze here the dispersion equation, which for an anisotropic plasma has the form (4.14). The plasma is assumed to be collisionless, i.e., the mean-field interaction dominates the system dynamics and $\nu=i0^+$. This assumption is correct if the inverse characteristic time of the mean-field phenomena τ^{-1} is substantially larger than the collision frequency ν. Otherwise, the infinitesimally small imaginary quantity $i0^+$ from (4.12) should be replaced by $i\nu$. Such a substitution, however, seriously complicates the analysis of the dispersion equation (4.14). Therefore, we solve the problem within the collisionless limit and only *a posteriori* argue that this approximation is valid.

As already mentioned, the solutions $\omega(\mathbf{k})$ of (4.14) are stable when $\mathrm{Im}\,\omega<0$ and unstable when $\mathrm{Im}\,\omega>0$. It appears difficult to find the solutions of Eq. (4.14) because of the complicated structure of the chromodielectric tensor (4.12). However, the problem simplifies because we are interested in the specific modes with the wave vector $\mathbf{k}$ perpendicular to, and the chromoelectric field $\mathbf{E}$ parallel to, the beam. Thus, we consider the configuration

$$\mathbf{E}=(0,0,E_z),\quad \mathbf{k}=(k_x,0,0). \tag{5.8}$$

Then the dispersion equation (4.14) takes the form

$$H(\omega)\equiv k_x^2-\omega^2\varepsilon^{zz}(\omega,k_x)=0, \tag{5.9}$$

where only one diagonal component of the dielectric tensor enters.

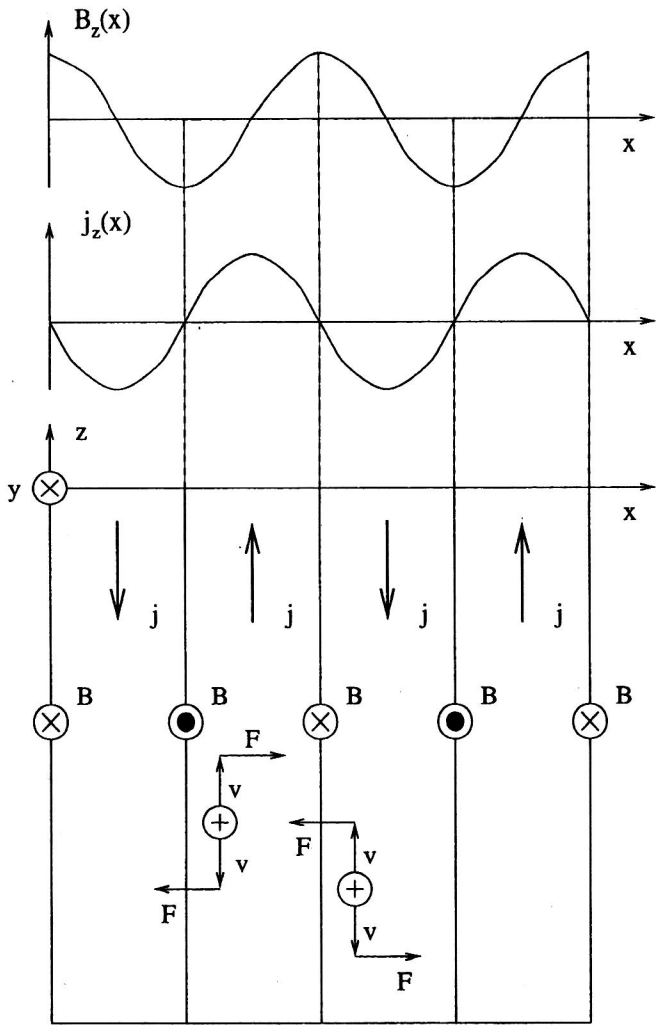

FIG. 4. The mechanism of filamentation. The phenomenon is, for simplicity, considered in terms of electrodynamics. The fluctuating current generates the magnetic field acting on the positively charged particles, which in turn contributes to the current (see the text). ⊗ and ⊙ denote the parallel and, respectively, antiparallel orientation of the magnetic field with respect to the y axis.

5.6. Penrose criterion

The stability analysis can be performed without solving Eq. (5.9) explicitly. Indeed, the so-called Penrose criterion[76] states that *the dispersion equation* $H(\omega)=0$ has *unstable solutions* if $H(\omega=0)<0$. The meaning of this statement will become clearer after we solve the dispersion equation approximately in the next subsection.

Let us compute $H(0)$, which can be written as

$$H(0)=k_x^2-\chi^2 \tag{5.10}$$

with

$$\chi^2\equiv-\omega_0^2=-\frac{g^2}{2}\int\frac{d^3p}{(2\pi)^3}\frac{v_z^2}{v_x}\frac{\partial f(\mathbf{p})}{\partial p_x}, \tag{5.11}$$

where the plasma-frequency parameter is

$$\omega_0^2\equiv-\frac{g^2}{2}\int\frac{d^3p}{(2\pi)^3}v_z\frac{\partial f(\mathbf{p})}{\partial p_z}. \tag{5.12}$$

As we shall see below, ω_0 gives the frequency of the stable mode of the configuration (5.8) when $k_x\to 0$.

Substituting the distribution functions (5.3) and (5.4) into Eqs. (5.11) and (5.12), one finds an analytic but rather complicated expression for $H(0)$. In the case of a flat y distribution, we thus take the limit $e^Y\gg 1$, while for a flat $p_\parallel$ distribution we assume that $\mathcal{P}\gg\langle p_\perp\rangle$. Then we get for a flat y distribution

$$\chi^2\cong-\frac{\alpha_s}{4\pi}\frac{e^Y}{Y}\int dp_\perp\left(h(p_\perp)+p_\perp\frac{dh(p_\perp)}{dp_\perp}\right)$$
$$=\frac{\alpha_s}{4\pi}\frac{e^Y}{Y}p_\perp^{\min}h(p_\perp^{\min}), \tag{5.13}$$

and for a flat $p_\parallel$ distribution

$$\chi^2\cong-\frac{\alpha_s}{4\pi}\mathcal{P}\int dp_\perp\frac{dh(p_\perp)}{dp_\perp}=\frac{\alpha_s}{4\pi}\mathcal{P}h(p_\perp^{\min}), \tag{5.14}$$

where $\alpha_s\equiv g^2/4\pi^2$ is the strong coupling constant and $p_\perp^{\min}$ denotes the minimal transverse momentum. The function $h(p_\perp)$ is assumed to decrease faster than $1/p_\perp$ when $p_\perp\to\infty$.

It can be seen that the sign of $H(0)$ given by Eq. (5.10) is (for sufficiently small k_x^2) determined by the transverse momentum distribution at the minimal momentum. There are unstable modes if $p_\perp^{\min}h(p_\perp^{\min})>0$ for the flat y distribution and if $h(p_\perp^{\min})>0$ for the flat $p_\parallel$ case. Since the distribution $h(p_\perp)$ is expected to be a monotonic decreasing function of $p_\perp$, the instability condition for the flat $p_\parallel$ distribution seems to be always satisfied. The situation for the flat y distribution is less clear. Thus, let us discuss it in more detail. We consider three characteristic cases of $h(p_\perp)$ discussed in the literature.

1. The transverse momentum distribution due to a single binary parton–parton interaction is proportional to $p_\perp^{-6}$ (Ref. 77) and blows up when $p_\perp\to 0$. In this case $p_\perp^{\min}h(p_\perp^{\min})>0$, there are unstable modes, and $p_\perp^{\min}$ should be treated as a cutoff parameter reflecting, e.g., the finite size of the system.

2. The transverse momentum distribution proportional to $(p_\perp+m_\perp)^{-6.4}$ with $m_\perp=2.9$ GeV has been found in Ref. 74, where the binary parton–parton scattering and the initial- and final-state radiation has been taken into account. This distribution, in contrast to that in case 1, gives $p_\perp^{\min}h(p_\perp^{\min})=0$ for $p_\perp^{\min}=0$, and there is no instability, although one should remember that the finite value of $m_\perp$ found in Ref. 74 is the result of infrared cutoff. Thus, it seems more reasonable to use the distribution in case 1, where the cutoff appears explicitly.

3. One treats perturbatively only partons with $p_\perp>p_\perp^{\min}$, assuming that those with lower momenta form colorless clusters or strings due to a nonperturbative interaction. It should be stressed that the colorless objects do not contribute to the dielectric tensor (4.12), which is found in the linear-response approximation.[7,66] Thus, only the partons with $p_\perp>p_\perp^{\min}$ are of interest for us. Consequently, $p_\perp^{\min}h(p_\perp^{\min})$ is positive, and there are unstable modes. As was shown in Ref. 72, the screening lengths due to the large parton density are smaller than the confinement scale in the

vacuum. Therefore, the cutoff parameter $p_\perp^{\min}$ should presumably be reduced from the value 1–2 GeV usually used for proton–proton interactions to, let us say, 0.1–0.2 GeV.

We cannot draw a firm conclusion, but we see that the instability condition is trivially satisfied for the flat $p_\parallel$ distribution, and is also fulfilled for the flat y distribution under plausible assumptions. Let us mention that the difference between the instability conditions for the flat y and $p_\parallel$ distributions is due to a very specific property of the y distribution, which is limited to the interval $(-Y,Y)$. The point is that $y\to\pm\infty$ when $p_\perp\to 0$, and, consequently, the limits in the rapidity suppress the contribution from the small transverse momenta to the dielectric tensor. For this reason we need for the instability the distribution $h(p_\perp)$ which diverges for $p_\perp\to 0$ in the case of the flat y distribution, while the instability condition for the flat $p_\parallel$ distribution is satisfied when $h(0)$ is finite. If we assumed the Gaussian rapidity distribution instead of (5.3), the instability condition would be less stringent. In any case, we assume that the Penrose criterion is satisfied and look for the unstable modes by solving the dispersion equation (5.9).

5.7. Unstable mode

The dispersion equation (5.9) for a cylindrically symmetric system is

$$k_x^2-\omega^2+\omega_0^2-\frac{\alpha_s}{4\pi^2}\int_0^\infty dp_\perp\int_{-\infty}^{\infty}\frac{dp_\parallel p_\parallel^2}{\sqrt{p_\parallel^2+p_\perp^2}}\frac{\partial f}{\partial p_\perp}\times\int_0^{2\pi}\frac{d\phi\cos\phi}{a-\cos\phi+i0^+}=0, \tag{5.15}$$

with the plasma frequency ω_0 given by Eq. (5.12) and a denoting the quantity

$$a\equiv\frac{\omega}{k_x}\frac{\sqrt{p_\parallel^2+p_\perp^2}}{p_\perp}.$$

We solve Eq. (5.15) in the two limiting cases $|\omega/k_x|\gg 1$ and $|k_x/\omega|\gg 1$. In the first case the azimuthal integral is approximated as

$$\int_0^{2\pi}\frac{d\phi\cos\phi}{a-\cos\phi+i0^+}=\frac{\pi}{a^2}+\mathcal{O}(a^{-4}).$$

Then Eq. (5.15) takes the form

$$k_x^2-\omega^2+\omega_0^2+\eta^2\frac{k_x^2}{\omega^2}=0, \tag{5.16}$$

where η, like ω_0, is a constant, defined as

$$\eta_0^2\equiv-\frac{\alpha_s}{4\pi}\int dp_\parallel dp_\perp\frac{p_\parallel^2 p_\perp^2}{(p_\parallel^2+p_\perp^2)^{3/2}}\frac{\partial f(\mathbf{p})}{\partial p_\perp}.$$

We have computed ω_0 and η for the flat $p_\parallel$ and y distributions. In the limits $e^Y\gg 1$ and $\mathcal{P}\gg\langle p_\perp\rangle$, respectively, we have found

$$\omega_0^2\cong\frac{\alpha_s}{8Y}\int dp_\perp h(p_\perp), \tag{5.17}$$

$$\omega_0^2\cong\frac{\alpha_s}{2\pi\mathcal{P}}\int dp_\perp p_\perp h(p_\perp) \tag{5.18}$$

and

$$\eta^2\cong\frac{\alpha_s}{16Y}\int dp_\perp\left(\frac{1}{4}h(p_\perp)-p_\perp\frac{dh(p_\perp)}{dp_\perp}\right), \tag{5.19}$$

$$\eta^2\cong-\frac{\alpha_s}{4\pi\mathcal{P}}\ln\left(\frac{\mathcal{P}}{\langle p_\perp\rangle}\right)\int dp_\perp p_\perp^2\frac{dh(p_\perp)}{dp_\perp}. \tag{5.20}$$

The solutions of Eq. (5.16) are

$$\omega_\pm^2=\frac{1}{2}(k^2+\omega_0^2\pm\sqrt{(k_x^2+\omega_0^2)^2+4\eta^2k_x^2}). \tag{5.21}$$

We see that $\omega_+^2\geqslant 0$ and $\omega_-^2\leqslant 0$. Thus, there is a purely real mode ω_+, which is stable, and two purely imaginary modes ω_-, one of which is unstable. As mentioned previously, $\omega_+=\omega_0$ when $k_x=0$.

Let us focus our attention on the unstable mode, which can be approximated as

$$\omega_-^2\cong\begin{cases}-\dfrac{\eta^2}{\omega_0^2}k_x^2 & \text{for } k_x^2\ll\omega_0^2,\\ -\eta^2 & \text{for } k_x^2\gg\omega_0^2.\end{cases}$$

One must bear in mind that Eq. (5.21) holds only for $|\omega/k_x|\gg 1$. We see that ω_- can satisfy this condition for $k_x^2\ll\omega_0^2$ if $\eta^2\gg\omega_0^2$ and for $k_x^2\gg\omega_0^2$ if $\eta^2\ll\omega_0^2$. To check whether these conditions can be satisfied, we compare η^2 with ω_0^2. Assuming that $h(p_\perp)\sim p_\perp^{-\beta}$, one finds, from Eqs. (5.19) and (5.20),

$$\eta^2\cong\frac{1+4\beta}{8}\omega_0^2,$$

$$\eta^2\cong\frac{\beta}{2}\ln\left(\frac{\mathcal{P}}{\langle p_\perp\rangle}\right)\omega_0^2. \tag{5.22}$$

Since $\beta\cong 6$ (Refs. 74 and 77), we get $\eta^2\geqslant 3\omega_0^2$. Therefore, the solution (5.21) for $k_x^2\ll\omega_0^2$ should be correct.

Let us now solve the dispersion equation (5.15) in the second case when $|k_x/\omega|\gg 1$. In this case the azimuthal integral in Eq. (5.15) is approximated as

$$\int_0^{2\pi}\frac{d\phi\cos\phi}{a-\cos\phi+i0^+}=-2\pi+\mathcal{O}(a),$$

and we immediately get the dispersion relation

$$\omega^2=k_x^2-\chi^2, \tag{5.23}$$

with χ^2 given by (5.13) or (5.14). As before, we have assumed that $e^Y\gg 1$ and $\mathcal{P}\gg\langle p_\perp\rangle$. Equation (5.23) provides a real mode for $k_x^2>\chi^2$ and two imaginary modes for $k_x^2<\chi^2$. Since the solution (5.23) must satisfy the condition $|k_x/\omega|\gg 1$, it holds only for $k_x^2\gg|k_x^2-\chi^2|$.

The dispersion relation for the unstable mode in the whole domain of wave vectors is shown schematically in Fig. 5, where the solutions (5.21) and (5.23) are combined. Now we see how the Penrose criterion works. When $\chi^2=0$, the unstable mode disappears.

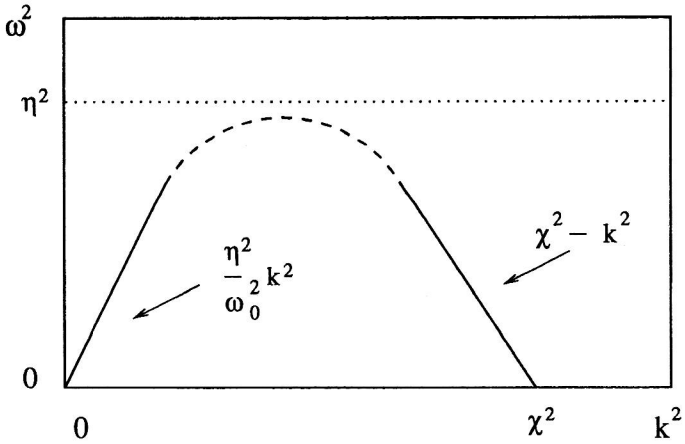

FIG. 5. Schematic view of the dispersion relation for the filamentation mode.

5.8. Time scales

The instability studied here can occur in heavy-ion collisions if the time of development of the instability is short enough—shorter than the characteristic time of evolution of the nonequilibrium state described by the distribution functions (5.3) and (5.4).

Let us first estimate the time of instability development given by $1/\mathrm{Im}\,\omega$. As can be seen in Fig. 5, $|\mathrm{Im}\,\omega|<\eta$. Thus, we define the minimal time as $\tau_{\min}=1/\eta$. To find $\tau_{\min}$ we estimate the plasma frequency. We consider here only the flat y distribution, which seems to be more reasonable than the flat $p_\parallel$ distribution. Approximating $\int dp_\perp h(p_\perp)$ as $\int dp_\perp p_\perp h(p_\perp)/\langle p_\perp\rangle$, the plasma frequency (5.12) can be written as

$$\omega_0^2 \cong \frac{\alpha_s \pi}{6 Y r_0^2 A^{2/3}}\left(N_q + N_{\bar q} + \frac{9}{4} N_g\right), \tag{5.24}$$

where $N_c=3$; N_q, $N_{\bar q}$, and N_g are the numbers of quarks, antiquarks, and gluons, respectively, produced in the volume, which has been estimated in the following way. Since we are interested in central collisions, the volume corresponds to a cylinder of radius $r_0 A^{1/3}$ with $r_0=1.1$ fm, where A is the mass number of the colliding nuclei. Using the uncertainty-principle argument, the length of the cylinder has been taken as $1/\langle p_\perp\rangle$, which is the formation time of a parton with transverse momentum $\langle p_\perp\rangle$.

Neglecting the quarks and antiquarks in Eq. (5.24) and substituting there $N_g=570$ for the central Au–Au collision at RHIC ($Y=2.5$) and $N_g=8100$ for the same colliding system at LHC ($Y=5.0$),[74] we get

$$\omega_0 = 280 \text{ MeV} \quad \text{for RHIC},$$

$$\omega_0 = 430 \text{ MeV} \quad \text{for LHC}$$

for $\alpha_s=0.3$ at RHIC and $\alpha_s=0.1$ at LHC. Using Eq. (5.22) with $\beta=6$, we find

$$\tau_{\min} = 0.4 \text{ fm}/c \quad \text{for RHIC},$$

$$\tau_{\min} = 0.3 \text{ fm}/c \quad \text{for LHC}.$$

The plasma has been assumed collisionless in our analysis. Such an assumption is usually correct for weakly interacting systems because the damping rates of the collective modes due to collisions are of higher order in α_s than the frequencies of these modes; see, e.g., Ref. 61. However, it has been argued recently[78] that the color collective modes are overdamped, owing to the unscreened chromomagnetic interaction. However, it is unclear whether these arguments apply to the unstable mode discussed here. The point is that Ref. 78 deals with the neutralization of color charges which generate the longitudinal chromoelectric field, whereas the unstable mode which we have found is transverse and consequently is generated by the color currents, not charges. Let us refer here to the electron–ion plasma, where the charge neutralization is a very fast process, while currents can exist in the system for a much longer time.[76] In any case, the above estimates of the instability development should be treated as lower limits.

Let us now discuss the characteristic time of evolution of the nonequilibrium state described by the distribution functions (5.3) and (5.4). Apart from the possible unstable collective modes, there are two other important processes responsible for the temporal evolution of the initially produced many-parton system: free streaming[79–81] and parton–parton scattering. The two processes lead to an isotropic momentum distribution of the partons in a given cell. The estimated time to achieve local isotropy due to free streaming is about $0.7\ \mathrm{fm}/c$ at RHIC.[81] The estimates of the equilibration time due to parton scatterings are similar.[82,83] We see that the three time scales of interest are close to each other. Therefore, the color unstable modes can play a role in the dynamics of a many-parton system produced at an early stage of a heavy-ion collision, but presumably the pattern of instability cannot fully develop.

5.9. Detecting the filamentation

One may ask whether the color instabilities are detectable in ultrarelativistic heavy-ion collisions. The answer seems to be affirmative because the occurrence of the filamentation breaks the azimuthal symmetry of the system and hopefully will be visible in the final state. The azimuthal orientation of the wave vector will change from one collision to another, while the growth of the instability will lead to energy transport along this vector (the Poynting vector points in this direction). Consequently, one expects significant

variation of the transverse energy as a function of the azimuthal angle. This expectation is qualitatively different from that based on parton cascade simulations,[59] where the fluctuations are strongly damped as a result of the large number of uncorrelated partons. Owing to the collective character of the filamentation instability, the azimuthal symmetry will presumably be broken by the flow of a large number of particles with relatively small transverse momenta. The jets produced in hard parton–parton interactions also break the azimuthal symmetry. However, the symmetry is broken in this case as a result of a few particles with large transverse momentum. The problem obviously needs further study, but the event-by-event analysis of the nuclear collision seems to give us a chance to observe the color instabilities in the experiments planned at RHIC and LHC.

*)E-mail: MROW@FUW.EDU.PL

1)The word *parton* is used as a common name for quarks and gluons.

2)We call the plasma *locally colorless* if the color four-current vanishes at each space-time point. This differs from the terminology used in electron–ion plasma physics, where the plasma is called *locally neutral* if the electric charge (zeroth component of the electromagnetic four-current) is everywhere zero.

3)This occurs when the characteristic mean-field frequency is much greater than the parton collision frequency.

4)We use units in which the fine-structure constant is $\alpha = e^2/4\pi$. In Gaussian units, which are traditionally used in electron–ion plasma physics, $\alpha = e^2$.

[1] F. J. Ynduráin, *Quantum Chromodynamics* (Springer-Verlag, New York, 1983).
[2] Proceedings of the Int. Conf. on Ultrarelativistic Nucleus–Nucleus Collisions, *Quark Matter '96*, Heidelberg, 1996, edited by P. Braun-Munzinger, H. J. Specht, R. Stock, and H. Stöcker (North-Holland, Amsterdam, 1996); Nucl. Phys. A **610**, (1996).
[3] S. R. de Groot, W. A. van Leeuwen, and Ch. G. van Weert, *Relativistic Kinetic Theory* (North-Holland, Amsterdam, 1980).
[4] H.-Th. Elze and U. Heinz, Phys. Rep. **183**, 81 (1989).
[5] J.-P. Blaizot and E. Iancu, Nucl. Phys. B **417**, 608 (1994).
[6] O. K. Kalashnikov, Fortschr. Phys. **32**, 525 (1984).
[7] St. Mrówczyński, Phys. Rev. D **39**, 1940 (1989).
[8] P. F. Kelly, Q. Liu, C. Lucchesi, and C. Manuel, Phys. Rev. D **50**, 4209 (1994).
[9] Yu. A. Markov and M. A. Markova, Teor. Mat. Fiz. **108**, 159 (1996) [in Russian].
[10] Yu. A. Markov and M. A. Markova, Teor. Mat. Fiz. **111**, 263 (1997) [in Russian].
[11] E. Braaten and R. D. Pisarski, Nucl. Phys. B **337**, 569 (1990).
[12] A. V. Selikhov, Phys. Lett. B **268**, 263 (1991).
[13] A. V. Selikhov and M. Gyulassy, Phys. Rev. C **49**, 1726 (1994).
[14] K. Geiger, Phys. Rev. D **54**, 949 (1996).
[15] Yu. A. Markov and M. A. Markova, Teor. Mat. Fiz. **103**, 123 (1995) [in Russian].
[16] J. Schwinger, Phys. Rev. **82**, 664 (1951).
[17] A. Białas and W. Czyż, Acta Phys. Pol. B **17**, 635 (1986).
[18] G. Gatoff, A. K. Kerman, and T. Matsui, Phys. Rev. D **36**, 114 (1987).
[19] F. Cooper *et al.*, Phys. Rev. D **48**, 190 (1993).
[20] Y. Kluger, J. M. Eisenberg, and B. Svetitsky, Int. J. Mod. Phys. E **2**, 333 (1993).
[21] J. Rau and B. Müller, Phys. Rep. **272**, 1 (1996).
[22] S. Schmidt *et al.*, hep-ph/9809227; Int. J. Mod. Phys. E (in press).
[23] J. Schwinger, J. Math. Phys. **2**, 407 (1961).
[24] L. V. Keldysh, Zh. Éksp. Teor. Fiz. **47**, 1515 (1964) [Sov. Phys. JETP **20**, 1018 (1965)].
[25] L. P. Kadanoff and G. Baym, *Quantum Statistical Mechanics* (Benjamin, New York, 1962).
[26] B. Bezzerides and D. F. Dubois, Ann. Phys. (N.Y.) **70**, 10 (1972).
[27] S.-P. Li and L. McLerran, Nucl. Phys. B **214**, 417 (1983).
[28] P. Danielewicz, Ann. Phys. (N.Y.) **152**, 239 (1984).
[29] E. Calzetta and B. L. Hu, Phys. Rev. D **37**, 2878 (1988).
[30] St. Mrówczyński and P. Danielewicz, Nucl. Phys. B **342**, 345 (1990).
[31] St. Mrówczyński and U. Heinz, Ann. Phys. (N.Y.) **229**, 1 (1994).
[32] P. Henning, Phys. Rep. **253**, 235 (1995).
[33] D. Boyanowsky, I. D. Lawrie, and D.-S. Lee, Phys. Rev. D **54**, 4013 (1996).
[34] S. P. Klevansky, A. Ogura, and J. Hüfner, Ann. Phys. (N.Y.) **261**, 37 (1997).
[35] P. Rehberg, Phys. Rev. C **57**, 3299 (1998).
[36] St. Mrówczyński, Phys. Rev. D **56**, 2265 (1997).
[37] P. Henning, Nucl. Phys. B **337**, 547 (1990).
[38] J. D. Bjorken and S. D. Drell, *Relativistic Quantum Fields* (McGraw-Hill, San Francisco, 1964).
[39] L. W. Nordheim, Proc. R. Soc. London, Ser. A **119**, 689 (1928).
[40] E. A. Uehling and G. E. Uhlenbeck, Phys. Rev. **43**, 552 (1933).
[41] U. Heinz, Phys. Rev. Lett. **51**, 351 (1983).
[42] J. Winter, J. Phys. (Paris) **45**, 53 (1984).
[43] H.-Th. Elze, M. Gyulassy, and D. Vasak, Nucl. Phys. B **276**, 706 (1986).
[44] H.-Th. Elze, M. Gyulassy, and D. Vasak, Phys. Lett. B **177**, 402 (1986).
[45] L. D. Landau and E. M. Lifshitz, *Electrodynamics of Continuous Media* (Pergamon, New York, 1960).
[46] V. P. Silin and A. A. Ruhadze, *Electrodynamics of Plasma and Plasma-like Media* [in Russian] (Gosatomizdat, Moscow, 1961).
[47] E. M. Lifshitz and L. P. Pitaevskiĭ, *Physical Kinetics* (Pergamon, New York, 1981).
[48] H.-Th. Elze, Z. Phys. C **38**, 211 (1987).
[49] U. Heinz and P. J. Siemens, Phys. Lett. B **158**, 11 (1985).
[50] U. Heinz, Ann. Phys. (N.Y.) **168**, 148 (1986).
[51] St. Mrówczyński, Phys. Lett. B **188**, 129 (1987).
[52] A. Białas and W. Czyż, Ann. Phys. (N.Y.) **187**, 97 (1988).
[53] A. Białłas, W. Czyż, A. Dyrek, and W. Florkowski, Nucl. Phys. B **296**, 611 (1988).
[54] U. Heinz, Ann. Phys. (N.Y.) **161**, 48 (1985).
[55] H. A. Weldon, Phys. Rev. D **26**, 1394 (1982).
[56] T. H. Hansson and I. Zahed, Nucl. Phys. B **292**, 725 (1987).
[57] U. Heinz, K. Kajantie, and T. Toimela, Ann. Phys. (N.Y.) **176**, 218 (1987).
[58] H. A. Weldon, Phys. Rev. D **28**, 2007 (1983).
[59] K. Geiger, Phys. Rep. **258**, 237 (1995).
[60] X.-N. Wang, Phys. Rep. **280**, 287 (1997).
[61] A. I. Akhiezer, I. A. Akhiezer, R. V. Polovin, A. G. Sitenko, and K. N. Stepanov, *Plasma Electrodynamics* (Pergamon, New York, 1975).
[62] U. Heinz, Nucl. Phys. A **418**, 603c (1984).
[63] Yu. B. Ivanov, Nucl. Phys. A **474**, 693 (1987).
[64] P. Henning and B. L. Friman, Nucl. Phys. A **490**, 689 (1988).
[65] Yu. E. Pokrovskiĭ and A. V. Selikhov, Pis'ma Zh. Éksp. Teor. Fiz. **47**, 11 (1988) [JETP Lett. **47**, 12 (1988)].
[66] St. Mrówczyński, Phys. Lett. B **214**, 587 (1988).
[67] Yu. E. Pokrovskiĭ and A. V. Selikhov, Yad. Fiz. **52**, 229 (1990) [Sov. J. Nucl. Phys. **52**, 146 (1990)].
[68] Yu. E. Pokrovskiĭ and A. V. Selikhov, Yad. Fiz. **52**, 605 (1990) [Sov. J. Nucl. Phys. **52**, 385 (1990)].
[69] O. P. Pavlenko, Yad. Fiz. **55**, 2239 (1992) [Sov. J. Nucl. Phys. **55**, 1243 (1992)].
[70] E. S. Weibel, Phys. Rev. Lett. **2**, 83 (1959).
[71] St. Mrówczyński, Phys. Lett. B **314**, 118 (1993).
[72] St. Mrówczyński, Phys. Rev. C **49**, 2191 (1994).
[73] St. Mrówczyński, Phys. Lett. B **393**, 26 (1997).
[74] T. S. Biró, B. Müller, and X.-N. Wang, Phys. Lett. B **283**, 171 (1992).
[75] F. F. Chen, *Introduction to Plasma Physics and Controlled Fusion* (Plenum Press, New York, 1984).
[76] N. A. Krall and A. W. Trivelpiece, *Principles of Plasma Physics* (McGraw-Hill, New York, 1973).
[77] K. J. Eskola, K. Kajantie, and J. Lindfors, Nucl. Phys. B **323**, 37 (1989).
[78] M. Gyulassy and A. V. Selikhov, Phys. Lett. B **316**, 373 (1993).
[79] R. Hwa and K. Kajantie, Phys. Rev. Lett. **56**, 696 (1986).
[80] T. S. Biró *et al.*, Phys. Rev. C **48**, 1275 (1993).
[81] K. J. Eskola and X.-N. Wang, Phys. Rev. C **47**, 2329 (1993).
[82] K. Geiger, Phys. Rev. D **46**, 4986 (1992).
[83] E. Shuryak, Phys. Rev. Lett. **68**, 3270 (1992).

This article was published in English in the original Russian journal. It is reproduced here with the stylistic changes by the Translations Editor.